Geophys. J. Int. (2003) **152,** 392–415

Analysis of long-term variations in the geomagnetic poloidal field intensity and evaluation of their relationship with global geodynamics

A. J. Biggin* and D. N. Thomas

Crustal Processes and Geodynamics Research Group, School of Earth Sciences & Geography, Kingston University, Penrhyn Road, Kingston-upon-Thames, Surrey, UK. E-mail: n.thomas@kingston.ac.uk

Accepted 2002 August 6. Received 2002 July 12; in original form 2001 June 13

SUMMARY

The 1167 published cooling unit (CU) palaeointensity estimates contained in the 400–10 Ma portion of the PINT global database were rigorously filtered according to accurate age determinations, palaeodirectional reliability, recognition of polarity and the method of palaeointensity acquisition. The remaining 865 estimates (group 1) were further filtered to ensure self-consistency, reducing the data set to 425 estimates (group 2). Group 1 and 2 data were clustered into temporally and/or spatially distinct rock suites (RS) enabling each part of the record to be assessed for potential biasing by overrepresentation of palaeosecular variation (PSV). The record was segmented according to the distribution of the data, rather than using arbitrary time windows, to ensure quasi-consistent behaviour within each segment. Differences between these segments clearly indicate that a significant long-timescale (10^7 and 10^8 yr) variation of the mean geomagnetic poloidal field intensity (GPFI) occurred during the 400–10 Ma period and hence that changing lowermost mantle conditions affect the capacity of the geodynamo to generate a poloidal field. Both the mean dipole moment and its standard deviation appear to be a function of the range of values each CU may adopt at one particular time. This range is itself controlled by the variation of the maximum limit of dipole moment, while the value of the minimum limit remains relatively constant. Tentative support is provided for the recent suggestion that PSV may have been reduced during the Cretaceous normal superchron (CNS), though more data are needed in the range 120–60 Ma to confirm this. No conclusive evidence was found to support the suggestion that the GPFI record may be biased towards low or high values by palaeointensity determinations obtained using methods that do not adopt pTRM checks. Indeed, offsets caused by unreliable data in well-represented parts of the record are likely to be random and cancel one another out.

When GPFI variation is analysed at a sufficiently high resolution to allow comparisons with the geomagnetic polarity reversal frequency (RF), it is not possible to confirm whether the two parameters are anticorrelated, decoupled or related in some more complex way. However, it is clear that GPFI and RF are definitely not positively correlated as has been previously suggested. The present database documents sharp increases in GPFI around the onset times of the two recognized superchrons, itself implying an anticorrelation. The implications, for geodynamo and mantle modelling, of both an anticorrelation and a decoupling of the geomagnetic parameters are discussed briefly.

A generic geodynamic model is proposed to explain the relationship between observed long-term changes in GPFI and global geodynamic processes. The model predicts that changes in GPFI result from a chain of geodynamic processes extending from crust to core, beginning with plate reorganizations at the surface and culminating in increases in the vigour of outer core convection. Supercontinents are transient surface expressions of such geodynamic processes and provide the potential to test the generic model. Four time stages are proposed to describe the major long-term changes in GPFI since the Early Devonian: 400–350, 350–250, 250–175

*Now at: Centro de Geociencias, UNAM Campus Juriquilla, Querétaro, 76230 Mexico.

© 2003 RAS

Downloaded from https://academic.oup.com/gji/article/152/2/392/653211 by guest on 04 February 2022

and 175–10 Ma. The GPFI features within these stages are convincingly explained within the context of major events in the evolutionary cycle of Pangaea. Two major avalanching and mantle reorganization events, facilitating whole-mantle convection, are proposed; one linked with the amalgamation of Pangaea, the other (possibly less catastrophic) with the dispersal phase of the supercontinent. These events were separated by a period of mantle insulation during the time when the supercontinent was assembled and a layered mantle convection regime existed. The explanations are consistent with independent evidence from seismology, mantle modelling and mantle dynamics, though some ambiguities and intriguing relationships remain, which can only be addressed by the addition of high-quality palaeointensity data in key time windows targeted by the statistical analysis. The potential of using GPFI variation from the Archaean to the Mid-Palaeozoic to enhance our understanding of Earth's early geodynamic evolution is highlighted. Such data are currently lacking and their acquisition represents a significant challenge for future palaeointensity work.

Key words: global geodynamics, palaeointensity variations, Pangaea evolution, reversal frequency.

Downloaded from https://academic.oup.com/gji/article/152/2/392/653211 by guest on 04 February 2022

1 INTRODUCTION

The Earth's magnetic field is a complex vector quantity for which both the magnitude (represented by geomagnetic palaeointensity, a measure of the poloidal component of the field strength) and the direction (represented by the geomagnetic polarity) vary over long ($>10^4$ yr) and short ($<10^4$ yr) timescales. Short-term variations result from geodynamo processes operating within the core (Dormy *et al.* 2000), whereas longer-term variations are believed to reflect the influence of lowermost mantle (LMM) processes on the geodynamo (McFadden & Merrill 1995). Therefore, links between long-term variations and mantle dynamic processes such as the formation of large igneous provinces (LIPs) and the variation in true polar wander (TPW) have been suggested (see Section 2). Previous attempts to evaluate these proposed links have concentrated on changes in geomagnetic polarity through geological time but have not rigorously considered palaeointensity variations. A major reason for this has been the availability of a detailed polarity record for much of the last 600 Myr (e.g. Johnson *et al.* 1995), coupled with a palaeointensity record that exhibits significant data paucity within critical time windows over the same period (e.g. Perrin & Shcherbakov 1997). The net result is that long-term trends in polarity have been identified, whereas the palaeointensity record has not, until recently, been comprehensive enough to enable any trends contained within it to be unequivocally identified. Nevertheless, the palaeointensity is fundamentally and intuitively linked with geodynamic processes. It is widely accepted that palaeointensity is related to the vigour of convection in the outer core (e.g. Buffet 2000) and, therefore, to the total heat flux out of the core across the core–mantle boundary (CMB; Buffet *et al.* 1996). This, in turn, is related to the temperature difference between the LMM and the outer core which is, itself, controlled by convection-induced cooling of the LMM resulting from the introduction of subducted, cool oceanic crust into the lower mantle following intense plate tectonic activity. Consequently, determination and interpretation of variations in palaeointensity (also termed geomagnetic poloidal field intensity, GPFI) through geological time should have a crucial bearing on our understanding of geodynamo behaviour and the geodynamic evolution of the Earth.

The present study aims to contribute to this understanding by conducting a rigorous statistical analysis of an enhanced global palaeointensity (PINT) database in order to identify any long-term trends in the data and to evaluate observations made by previous studies of the published database. A model is proposed to interpret the features documented in the record within the context of global-scale geodynamic processes, taking into account evidence from other geoscientific studies such as seismic imaging of the mantle, mantle dynamics and tectonic observations.

2 RELATIONSHIP BETWEEN GEOMAGNETIC VARIABLES AND GEODYNAMIC PROCESSES

2.1 Long-term variations in the direction (polarity) of the geomagnetic field

A fundamental feature of the geomagnetic field is its ability to reverse polarity. The record of polarity reversals is very well documented back to 160 Ma (e.g. Cande & Kent 1995) and quasi-continuous back to 330 Ma (Opdyke & Channell 1996), beyond which the record becomes more ambiguous. However, Johnson *et al.* (1995) produced a record of reversal frequency with time showing that, over the past 600 Myr, the reversal frequency is clearly non-stationary. There are two well-defined periods (320–260 Ma: the Permo-Carboniferous reverse superchron, PCRS and 120–80 Ma: the Cretaceous normal superchron, CNS) when the reversal process ceases. During these superchrons the geodynamo processes accounting for the occurrence of reversals are clearly suppressed. McFadden & Merrill (1997) reported that the reversal frequency was asymmetric about the CNS, with the fall prior to the onset of the superchron being steeper than the recovery after its termination. They interpreted this as indicating that the geodynamo lost energy at a faster rate before a superchron than it regained energy after one. The reversal frequency increased sharply after the end of the PCRS and continued to rise gradually through the Triassic but data leading into the PCRS are too sparse to establish, for certain, the nature of the decrease in reversal frequency. There is a suggestion that a third superchron, the Ordovician reverse superchron (OrRS), existed between approximately 500 and 460 Ma (Johnson *et al.* 1995). However, insufficient data coverage in comparison with the other two superchrons has meant that this feature has yet to be confirmed and, indeed, some sources (e.g. Torsvik *et al.* 1995) believe that inadequate sampling of both polarities produces a reverse polarity bias in this age range creating a 'ghost' superchron.

The overturn time of the core is ~500 yr and the longest timescale operating in the core is ~5000 yr (Gubbins 1999). Therefore, it is clear that changes in the core cannot be responsible for the

long-term trends witnessed in the polarity record. Such trends are likely to result from changes in CMB conditions that are controlled by circulation in the lowermost mantle (McFadden & Merrill 1995). By logical extension of this argument, changes in the lithosphere have been linked with changes in geomagnetic polarity. Early attempts to explain the link between geomagnetic variations and lithospheric processes centred on the correlation of geomagnetic reversal frequency with intraplate volcanism (e.g. Vogt 1972; Jones 1977; Loper & McCartney 1986). These models were later found to be mostly based on spurious data (Merrill *et al.* 1996), but formed the basis for the idea that thickness changes in the CMB region, and subsequent release of mantle plumes, triggered shifts in the reversal frequency. Larson (1991) attributed a 50–75 per cent rise in oceanic crust production from 120 to 80 Ma to the existence of a superplume originating from the CMB region. Larson & Olson (1991) proposed that thinning of D″, resulting from the release of a superplume, increased the heat flux across the CMB and therefore increased core convection, triggering the onset of the CNS. However, Loper (1992) showed that a plume typically takes 20–30 Myr to reach the surface from the CMB, which is too long to explain the coincidence of the CNS with increased crustal production. Larson & Kincaid (1996) modified the model by suggesting that subducted slabs, from the breakup of Gondwanaland, penetrated the 660 km boundary layer, causing its upward advection because of counter-flow and resulting in surface volcanism. This volcanism was, coincidentally, synchronous with the arrival of the slab at the CMB, which triggered the change in heat flux and the onset of the CNS.

Eide & Torsvik (1996) linked a standstill in the reversal frequency (represented by the PCRS) with the amalgamation of Pangaea. Ponding of slabs at the 660 km layer during the accretion of Pangaea and subsequent avalanching through the mantle resulted in material arriving at the CMB and spreading along it to produce a 'cold blanket'. This led to an increase in heat flow across the CMB and triggered the superchron at ∼320 Ma. Courtillot & Besse (1987) and Besse & Courtillot (1991) compared reversal frequency with true polar wander (TPW), finding that TPW was lowest during periods when reversal frequency was reducing and, conversely, highest when the reversal frequency was increasing and the mantle was more active. Again, the causative link was a plume emitted from a thick D″. Courtillot & Besse (1987) also showed that reversals may be triggered by sinking of material from the base of the CMB into the outer core, the so-called 'cold blobs' proposed by McFadden & Merrill (1986). Such instabilities would be more likely to exist when D″ was thick.

The relevance of mantle plumes to the whole issue is unclear. There is some doubt concerning the extent to which plumes generated at D″ could influence a dominantly subduction-driven convecting regime (Griffiths & Turner 1998; Anderson 1994; Anderson 1998; Heller *et al.* 1996; Sheth 1999; Dalziel *et al.* 2000). Courtillot *et al.* (1999) recently proposed that a combination of 'active' (plume-related) and 'passive' (lithospheric weakness-related) rifting to link the formation of flood basalts and continental fragmentation but, in all cases, a plume is a pre-requisite for breakup. Loper (1992) suggested that the response time of CMB heat flux to the emission of a plume would be comparable to the age of the Earth. Consequently, such processes could not be responsible for the observed variations in the reversal record.

Prévot *et al.* (2000) also analysed the link between reversal frequency and TPW. They noted a peak in TPW at ∼ 110 Ma, which is coincident with increased volcanism and suppressing of the reversal frequency. They interpreted this as being a signal of a major mantle reorganization in the Early Cretaceous where avalanching of material through the 660 km layer marked the cessation of layered convection that existed prior to, and after, the '110 Ma event'. However, Tarduno & Smirnov (2001) regard the '110 Ma event' to be an artefact of Atlantic hotspot activity. In their view, the mantle reorganization event was not rapid enough to drive TPW. A recent study by Torsvik *et al.* (2001) provided some support for the Prévot *et al.* (2000) model (see Section 7 for further discussion).

One of the more compelling pieces of evidence linking reversal frequency with lithospheric processes comes from the wavelet analysis of the reversal record by Ricou & Gibert (1997). They show that each of the ten discrete discontinuities in the reversal record over the past 160 Myr corresponds to the formation or abandonment of a major MOR, with a time delay of only 3 Myr. This close correlation can only be explained by direct coupling between the CMB and the lithosphere. They suggest that lateral changes in mass distribution at the surface (through plate reorganization) are mirrored by similar changes in mass distribution on the CMB, though they did not discuss potential mechanisms. This remains one of the only lines of evidence linking the core with the crust without requiring the long-timescale transfer through the whole mantle.

2.2 Relationship between palaeointensity and geodynamic processes

Buffet (2000) noted that the vigour of core convection, and therefore the strength of the geodynamo, is influenced by the heat flow across the CMB. However, the paucity of the palaeointensity record and our consequent inability to identify long-term trends with any significant confidence has precluded, until now, any rigorous analysis of the relationship between observed palaeointensity and geodynamic processes. Nevertheless, within the context of evaluating links between the existence of superchrons and mantle plume activity, Loper & McCartney (1986) and Larson & Olson (1991) suggested that production of mantle plumes thins D″ and increases the heat flux across the CMB, thereby increasing the energy supplied to the geodynamo and, consequently, strengthening the geomagnetic field. They disagree, however, on the relationship between palaeointensity and reversal frequency. Loper & McCartney (1986) suggest that the field intensity should be low during superchrons, whereas Larson & Olson (1991) favour high field strength during periods of constant polarity. Others (e.g. Prévot *et al.* 1990; Thomas *et al.* 1998, 2000) suggest no simple relationship between these geomagnetic features and favour the decoupling of processes controlling reversal frequency and palaeointensity. If true, this would provide an important constraint on attempts to model geodynamo behaviour (see Section 5.2 for further discussion). Despite the lack of agreement, it is accepted that any long-term changes in the geomagnetic field intensity record are clearly linked to lowermost mantle processes and, by logical extension of this argument, to a chain of geodynamic events. The present study proposes a model (Section 6.1) where this chain originates with mass redistribution at Earth's surface and culminates in changes in the pattern of outer core convection.

3 THE GLOBAL PALAEOINTENSITY RECORD

3.1 Introduction

Absolute estimates of the geomagnetic poloidal field intensity are derived, experimentally, from the thermoremanent magnetization (TRM) acquired by rocks as they cool down through the Curie temperatures of their constituent magnetic minerals. The (palaeo)intensity of the TRM is, ideally, directly proportional to that of the ambient field at the time of rock cooling. A palaeointensity

Downloaded from https://academic.oup.com/gji/article/152/2/392/653211 by guest on 04 February 2022

result is then used in conjunction with a palaeomagnetic inclination to calculate a virtual dipole moment (VDM; Smith 1967), allowing a direct comparison of results from different localities. In practice, palaeointensity determination is often hindered by thermal alteration of samples during successive heating that either significantly reduces the success rate of experiments, or introduces an element of doubt into seemingly successful determinations. Significant advances in palaeointensity methodology (techniques and sample selection) since the original Thellier technique was first introduced (Thellier & Thellier 1959) have progressively increased our ability to recover palaeointensity results from ancient rocks and have enhanced confidence in the results obtained (Coe 1967; Coe *et al.*1978; Prévot *et al.*1985; Pick & Tauxe 1993; Thomas 1993; Juárez *et al.*1998). So-called pTRM checks can now monitor thermal alteration during progressive heating and isolate usable temperature ranges, over which the sample is not adversely affected, allowing palaeointensities to be determined. The most recent technology utilizes microwaves to directly excite magnons within the magnetic material of a sample (Walton *et al.* 1992, 1993, 1996) so that, in microwave Thellier experiments, the sample is heated to much lower temperatures than it would be in a conventional oven. This significantly reduces sample alteration and has been demonstrated to yield success rates equivalent to, or better than, conventional Thellier analyses on historic and ancient igneous rocks (Hill & Shaw 1999, 2000; Hill *et al.* 2002). The most impressive indication of the potential of the new microwave Thellier technique to date recorded a 58 per cent success rate from sister samples of Tertiary basaltic material that yielded no conventional Thellier results (Hill *et al.* 2002).

These advances have facilitated the successful determination of palaeointensities from rocks dating back to 3.5 Ga. As a result, the global palaeointensity (PINT) database, originally compiled by Tanaka *et al.* (1995), has grown rapidly leading to subsequent updates by Perrin & Shcherbakov (1997) and Perrin *et al.* (1998).

3.2 Previous statistical analyses

Previous statistical analyses of the entire record, or large parts of it (Kono & Tanaka 1995; Perrin & Shcherbakov 1997; Selkin & Tauxe 2000) yielded the following observations.

(1) At present, the VDM data set does not clearly display any overall trend with time since 3.5 Ga (Kono & Tanaka 1995).

(2) Much of the Mesozoic is characterized by persistently low dipole moment values (~30 per cent of present-day values). This so-called Mesozoic dipole low (MDL) was first reported by Prévot *et al.* (1990) and has subsequently been confirmed by numerous studies. Its boundaries and the nature of transition between the MDL and the present dipole state are, as yet, unclear (e.g. Thomas *et al.* 1998, 2000). Perrin & Shcherbakov (1997) demonstrated that the dipole structure of the field was maintained through this period and that the MDL is unlikely to be an artefact of insufficient sampling of a Neogene-type field.

(3) Secular variation (SV) of the field is much greater for the period 10–0 Ma than for 10–0 Kyr (Kono & Tanaka 1995), suggesting that most dipole field fluctuations occur over a period of $\geq 10^4$ yr. Perrin & Shcherbakov (1997) showed that 10 Myr averages of the field for the last 300 Myr illustrated a direct relationship between the mean VDM and its standard deviation.

(4) Selkin & Tauxe (2000) performed the most recent analysis of the global dipole moment record prior to this study. They only accepted estimates that were produced using the Thellier method with pTRM checks (T+ results). They concluded that there was no long-term dipole moment variation between 0.3 and 300 Myr and that a mean value of $\sim 5 \times 10^{22}$ A m^2 was maintained.

4 ANALYSIS USED IN THIS STUDY

4.1 Data selection and overview

The initial data set used in this study comprises the PINT database described by Tanaka *et al.* (1995), Perrin & Shcherbakov (1997) and Perrin *et al.* (1998) enhanced at the time of submission using a reference list kindly provided by Mireille Perrin. The pooled set contained nearly 2600 cooling unit (CU) palaeointensity estimates but the following filtering steps were applied to allow the study to focus on analysing trends of 10^7–10^8 yr and to remove unreliable and unusable data.

(1) An age between 10 and 400 Myr, either of radiometric or stratigraphic origin must be specified. The period 10–0 Ma contains 29 per cent of the PINT data, is heavily skewed towards the 5–0 Ma age range and been rigorously studied by Kono & Tanaka (1995). Therefore, it was decided that these data would be omitted. Conversely, data from rocks older than 400 Myr are very scarce and sufficiently widely distributed to render an analysis, even of 10^8 yr trends, untenable and are therefore omitted.

(2) A VDM or VADM must be calculated from either the inclination of the magnetization or inferred from palaeolatitude. This allows palaeointensity results from different locations on the globe to be compared directly.

(3) The polarity of magnetization must not be specified as transitional. The strength of the poloidal field is believed to fall substantially for several thousand years during a geomagnetic polarity transition (e.g. Prévot *et al.* 1985) which is not a facet of the long-term variation under investigation.

(4) The method of palaeointensity acquisition must be either modified Thellier or Shaw or a combination using one or both of these methods. The Thellier method is widely regarded as the most reliable method of estimating palaeointensity (Prévot *et al.* 1990; Prévot & Perrin 1992). The modified Shaw method (Shaw 1974; Rolph & Shaw 1985), although lacking support from some workers and prone to producing estimates with large scatter, has been shown in practice to give similar results to the Thellier method (e.g. Thomas 1992). Data acquired using this method were also considered acceptable in the analysis performed by Kono & Tanaka (1995).

Following the application of the four-stage filter outlined above, 865 CU estimates remained on which to perform the analysis. This set (referred to as group 1 hereafter) contained no data known to be unreliable or inappropriate. Self-consistency is an important quality for site averages to display: a CU is generally produced from sample estimates close to one another in a rock unit and therefore should not be subject to variation of geomagnetic origin. Consequently, CU data within group 1 produced by averaging three or more individual estimates and with a corresponding standard deviation of 10 per cent or less were elevated to group 2 status. A total of 425 CU data satisfied these criteria.

Virtually all recent absolute palaeointensity studies have used the modified Thellier method with sliding pTRM checks (Coe 1967; Prévot *et al.* 1985). The pTRM checks provide a method of monitoring an alteration that would not reveal itself in changes of the slope of the NRM–TRM plot. Because of the safeguard provided by these checks, those group 2 CU data that were acquired using this method (the so-called T+ estimates) were further elevated to group 3 status. The 47 CU estimates in the group 3 subset (amounting to

Downloaded from https://academic.oup.com/gji/article/152/2/392/653211 by guest on 04 February 2022

only ∼5 per cent of the group 1 data and ∼ 11 per cent of the group 2 data set) therefore represent the most reliable available data, according to conventional wisdom. However, a few caveats apply and such estimates should not be considered as perfectly reliable. Although laboratory-induced alteration is largely protected against in T+ estimates, other problems that affect palaeointensity accuracy are not. First, samples retaining a remanence that is not thermal in origin can produce seemingly reliable but low palaeointensity estimates (Goguitchaichvili *et al.* 1999) when this method is used. Secondly, pTRM checks will be shown by Biggin & Thomas (2002, submitted) to offer no protection against concave-up NRM–TRM plots that are sometimes produced by samples with pseudo-single-domain bulk hysteresis properties. The effect of the latter phenomenon is usually to produce an incorrect, high-palaeointensity estimate (for examples, see Calvo *et al.* 2002).

Overrepresentation of palaeosecular variation (PSV) is a potential problem for statistical analysis of the palaeointensity record. To allow the extent of this problem to be assessed, all CU data were grouped into temporally and/or spatially distinct units termed rock suites (RS). Each of these incorporates all estimates acquired within ±5° latitude and longitude of one another at times less than 5 Myr apart and with uncertainties in the age determination allowing them to have been magnetized synchronously. These limits are wholly arbitrary but do ensure that each RS is a spatially and/or temporally distinct estimate of GPFI. The full CU and RS data sets for all three groups, together with their source references are available on-line at http://www.kingston.ac.uk/esg/geophysics.

This study attempts to overcome the problems associated with PSV by developing the concept of rock suites so that potentially problematic time periods in the record can be identified. This technique is very different from that used recently by Tarduno *et al.* (2001) who only accepted groups of estimates that together comprise a palaeomagnetic dipole moment (PDM) with associated palaeodirectional data suggesting that the secular variation is averaged. Our technique is justified on practical grounds: very few published palaeointensity studies claim to produce a PDM and therefore the approach adopted by Tarduno *et al.* (2001) requires that a large quantity of otherwise reliable estimates is discarded. This would render an analysis of the type used in the present study untenable. The technique used here allows an assessment of potential risks without losing a considerable amount of information.

Table 1 indicates that the means of the groups 1 and 3 data sets are similar, whereas that of group 2 is somewhat higher. Fig. 1 provides an insight into the reason for this: a clear bimodality is evident in the distribution of group 2 data with a secondary peak at approximately 10×10^{22} A m^2, which is suppressed in both the groups 1 and 3 distributions. Perrin & Shcherbakov (1997) observed a bimodal distribution for their selected data set and remarked that a non-monotonic variation in intensity is not atypical of a highly nonlinear system such as the geodynamo. However, we noted that a significant proportion (36 per cent) of our group 2 subset of CU estimates comprised data from just three large rock suites (RS numbers 74, 81 and 90 in the on-line list) all derived from Russia and Uzbekistan with ages just prior to or during the Permo-Carboniferous reverse superchron. When these estimates, which have generally high values, are removed from group 2, this secondary peak in the distribution disappears (Fig. 1d). Therefore, the likely explanation for the bimodality is an overrepresentation of a particular period of GPFI behaviour.

Table 1. Basic statistical parameters for the three groups defined in the text. μ_{VDM} and σ_{VDM} are the overall means and standard deviations in units of 10^{22} A m^2. N_{CU} and N_{RS} refer to the number of cooling unit estimates and the number of rock suite groups, respectively.

Group	μ_{VDM}	σ_{VDM}	N_{CU}	N_{RS}
1	5.9	3.5	865	89
2	3.3	3.1	425	44
3	5.8	3.2	47	16

The underlying distributions of all three groups are closer to lognormal than Gaussian. This has been reported previously for populations of palaeointensity data (McFadden & McElhinny 1982; Kono & Tanaka 1995), although a gamma distribution has been argued to produce a better fit (Constable *et al.* 1998). Unfortunately, the highly variable age distribution of the CU estimates (Fig. 2) precludes any meaningful analyses to ascertain the underlying distributions of entire group populations in this study.

The oldest CU estimates from group 3 are dated at 301 Myr. The other two groups were truncated above this age and have cumulative distribution functions (CDFs) of their ages and dipole moments plotted together with those of group 3 in Fig. 3. The CDFs for the three ages (Fig. 3a) differ from one another significantly but, surprisingly, the CDFs of the VDM distribution (Fig. 3b) for each are remarkably similar. The non-parametric Kolmogorov–Smirnov test, as used and described by Selkin & Tauxe (2000), was used here to compare the VDM distributions of the group 1 and 3 populations as these had the closest age distributions. The test could not rule out the null hypothesis that the two populations were samples of the same distribution at the 95 per cent confidence level.

Fig. 4 shows plots of CU estimates and rock suites from all three groups through time. Those of group 1 and 2 data share some qualitative similarities as listed below.

(1) Large temporal gaps exist in many parts of the record but these become more frequent and extensive in older parts.

(2) Between the Middle Carboniferous and the end of the Permian (325–245 Ma), the CU data are controlled by fewer, larger rock suites than are present in other time periods. Throughout this time, the mean dipole moment appeared to decrease in an almost linear fashion.

(3) For most parts of the record, the variation in the highest values of both CU and RS data is much greater than the variation in the lowest values over periods of 10^7–10^8 yr.

(4) From the Middle Jurassic to the Early Cretaceous (∼170–120 Ma) there is an absence of high ($>8 \times 10^{22}$ A m^2) CU estimates and a concentration of low ($<5 \times 10^{22}$ A m^2) values. The average value appears to rise from this period to some maximum between 50 and 10 Ma.

(5) Throughout the Devonian and Early Carboniferous, the dipole moment appeared to remain low.

Unfortunately, the distribution of group 3 data through time as shown in Fig. 4(c) is insufficient to allow any general observations to be made. There are real dangers of aliasing and overrepresentation of PSV as demonstrated by the limited coverage of CU and RS data, respectively. Consequently, the statistical analysis from hereon will focus on the group 1 and 2 data sets. However, some analysis of group 3 data will be given in Section 4.4.

Most of the observations given above have been noted in previous studies (see Section 3.1). The intention of the first part of this study is to assess the validity of the observations and clarify the work needed to improve our confidence in them.

Downloaded from https://academic.oup.com/gji/article/152/2/392/653211 by guest on 04 February 2022

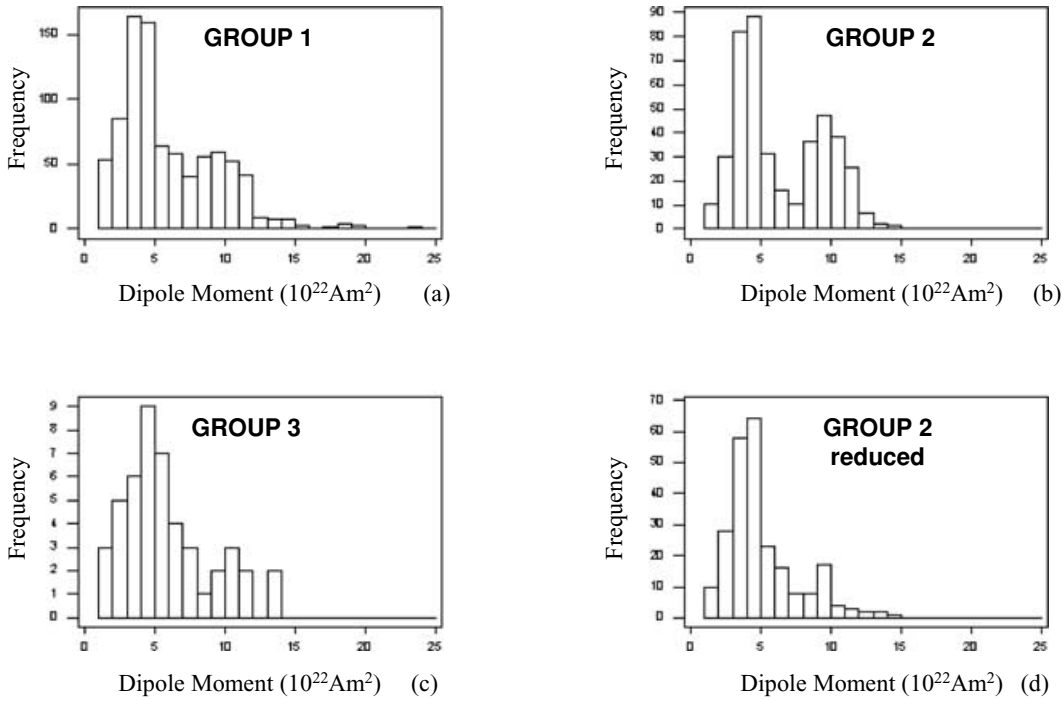

Figure 1. (a)–(c) Histograms showing dipole moment distributions for the three groups as indicated. Part (d) shows the distribution of group 2 data set after data drawn from three rock suites are omitted (see the text for details).

4.2 Segments within the record

In order to assess long-term temporal variation in GPFI, the dipole moment records were segmented. Instead of the usual practice of applying an arbitrary window (e.g. 10 Myr), it was decided that the boundaries of the segments should be prescribed by the distribution of the data themselves so that there was quasi-consistent behaviour within each segment.

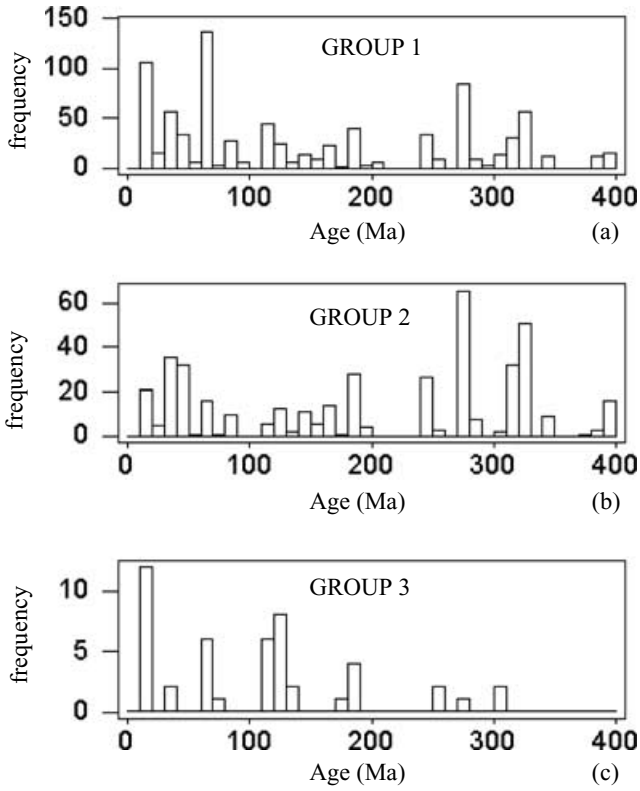

Figure 2. Histograms showing the age distribution of data in each of the three groups.

Fig. 4 suggests that mean dipole moment values have risen since the Middle Jurassic (during the period 172–10 Ma, as defined by group 1 data). This was confirmed by the application of a simple regression to the CU data in this period that rejected the null hypothesis of a zero slope (i.e. a random distribution through time) with greater than 99 per cent confidence for both group 1 and 2 data.

Analysis of variance (ANOVA) is an effective means of assessing the difference between random samples taken from different populations by comparing the variance within and between each population. To determine whether the progression of GPFI was continuous or punctuated, the probability of rejecting the null hypothesis provided by the regression (i.e. the likelihood of gradual change) was compared with the probabilities calculated using the ANOVA technique (i.e. the likelihood of punctuated change) on a range of iterated segments. This was achieved first by imposing only one segment partition on the 172–10 Ma series and performing ANOVA (with a null hypothesis of equal population means in each segment) iteratively as the partition was shifted through time. Subsequently, the two most significant segments were analysed separately and further partitions could be introduced. Partitioning was halted when a smooth change was preferred to a definite transition within a segment or no change was evident.

The optimum configuration of the partitions through the entire period was observed to be very similar prior to the Tertiary for both group 1 and 2 data sets and a significant improvement on the single regression model was evident in both cases. Each data set had four partitions (Fig. 5) and the ages of two of these (the Late Jurassic and Early Cretaceous) were common to both data sets. The two other partitions for group 1 were located in the Early Miocene and Late Eocene (Fig. 5a), while those for group 2 were in the Mid-Late Eocene and the Late Palaeocene–Early Eocene (Fig. 5b).

Downloaded from https://academic.oup.com/gji/article/152/2/392/653211 by guest on 04 February 2022

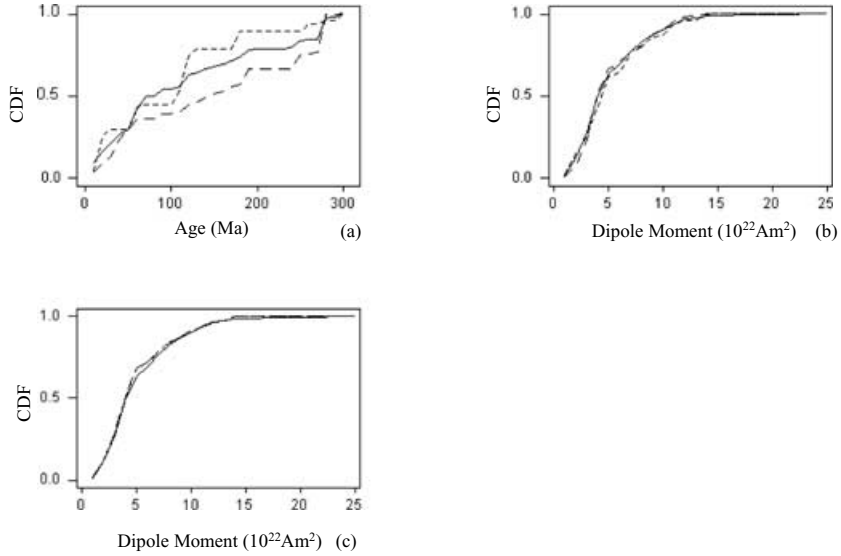

Figure 3. (a) Cumulative distribution functions (CDFs) of ages for group 1 (solid line), group 2 (long dashes) and group 3 (short dashes) data sets truncated above 301 Ma. (b) CDFs of dipole moment values for the 3 data sets. (c) CDFs of dipole moment values for the group 1 data set (solid line) truncated above 301 Ma and the data derived using the selection criteria of Selkin & Tauxe (2000) (broken line).

Some basic statistical parameters for each of the segments are shown in Tables 2 and 3. Segment 3 in particular suffers from a paucity of estimates in its interior so that the regression line within it tends to be 'anchored' to data concentrated at its margins (Fig. 5). Nevertheless, the slopes of these for both group 1 and 2 data in the two later segments are equal to or less than $\pm$ 0.01 $\times$ 10^{22} A m^2 Myr^{-1} and therefore the null hypothesis of no variation could not be rejected at any reasonable confidence level. This suggests that there was little *overall* evolution of the mean dipole moment through this period of time.

The other segments shown in Fig. 5 do not have sufficient temporal coverage to allow a discussion of their internal behaviour. It is stressed that neither the group 1 nor group 2 model outlined above, and illustrated in Figs 5 and 7 and Tables 2 and 3, is intended as a final interpretation of GPFI since the Middle Jurassic. Large gaps in the record still exist and the calculated positions of the partitions are particularly sensitive to CU data close to them. However, the main objective of the ANOVA analysis was to allow this part of the record to be segmented meaningfully and this was achieved.

Segmentation of the rest of the record in the same manner was not undertaken because large temporal breaks and the limited number of rock suites (evident by the dominance of vertical strips of data in the CU records) meant that the sampling distribution itself would have generated the partitions. Instead, the partitions were introduced by eye with the objective of generating segments within which behaviour was quasi-consistent (Fig. 6 and Tables 2 and 3).

The data from the generated segments (Fig. 7) clearly display trends in mean dipole moment for both groups of data. However, the segments from before the Middle Jurassic can be treated with less confidence because of the generally lower number of rock suites per segment (Tables 2 and 3) and the larger gaps between them (Figs 5 and 6). The trends are broadly similar for both group 1 and 2 data sets, with the only noteworthy differences occurring after 50 Ma when group 1 exhibits a rise, whereas group 2 shows the opposite. Segment number 9 (301–290 Ma) in Fig. 7(b) can all but be ignored because it is comprised of only two CU data.

The standard deviation, shown as error bars in Fig. 7, supports the idea that it is the variation in the upper limit of the range of values the dipole moment can adopt in a period of time that controls the mean value. The lower limit appears to remain fairly constant regardless of the mean. Two obvious corollaries of this are that it is the variation of the highest values that dominantly control the mean and that the magnitude of shorter-term ($<10^7$ yr) variation is proportional to the mean value. The exceptions to this rule are segment number 11 (325–310 Ma) for both groups of data and segment number 2 (49.5–46.5 Ma) for group 2 only. Both these segments have high means but low standard deviations. However, this could be because they are both comprised of only two rock suites and the very short age range of segment 2 from group 2 should also be noted. Obviously more high-quality, spatially distributed data are required before the unusual behaviour of these two segments can be verified as true features of GPFI variation.

20 random samples of group 2 CU estimates were taken from nine of the segments, in order to normalize Nso that their mean dipole moment and associated standard deviation could be compared with those of segment number 4 (143.5–123 Ma). This was undertaken in order to investigate the suspicion that the relationship between the mean and standard deviation is a consequence of the number of data comprising the mean. These are plotted in Fig. 8 and it is immediately obvious that, while segment numbers 2 and 10 are significant outliers, there is otherwise a clear tendency for the standard deviation of a segment to increase with its mean. Although the number of cooling units (N_{CU}) has been normalized for all the segments, there could still be a suspicion of statistical biasing if the standard deviation was proportional to the number of rock suites, N_{RS} (or the ratio $N_{\mathrm{RS}}/N_{\mathrm{CU}}$) within the segment. However, Table 3 shows that this is clearly not the case.

The means of the 20 mean and standard deviation values taken from each of the eight non-outlying segments are also plotted in Fig. 8. A regression applied to these rejects the null hypothesis of no relationship at the 99 per cent confidence limit and produces the best-fitting line shown. However, this quasi-linear relationship definitely does not go to the origin, but rather intercepts the mean dipole moment axis at approximately 1.5 $\times$ 10^{22} A m^2. Significantly, this means that the ratio of the standard deviation to the mean value will be lower for low values of mean dipole moment than for high

Downloaded from https://academic.oup.com/gji/article/152/2/392/653211 by guest on 04 February 2022

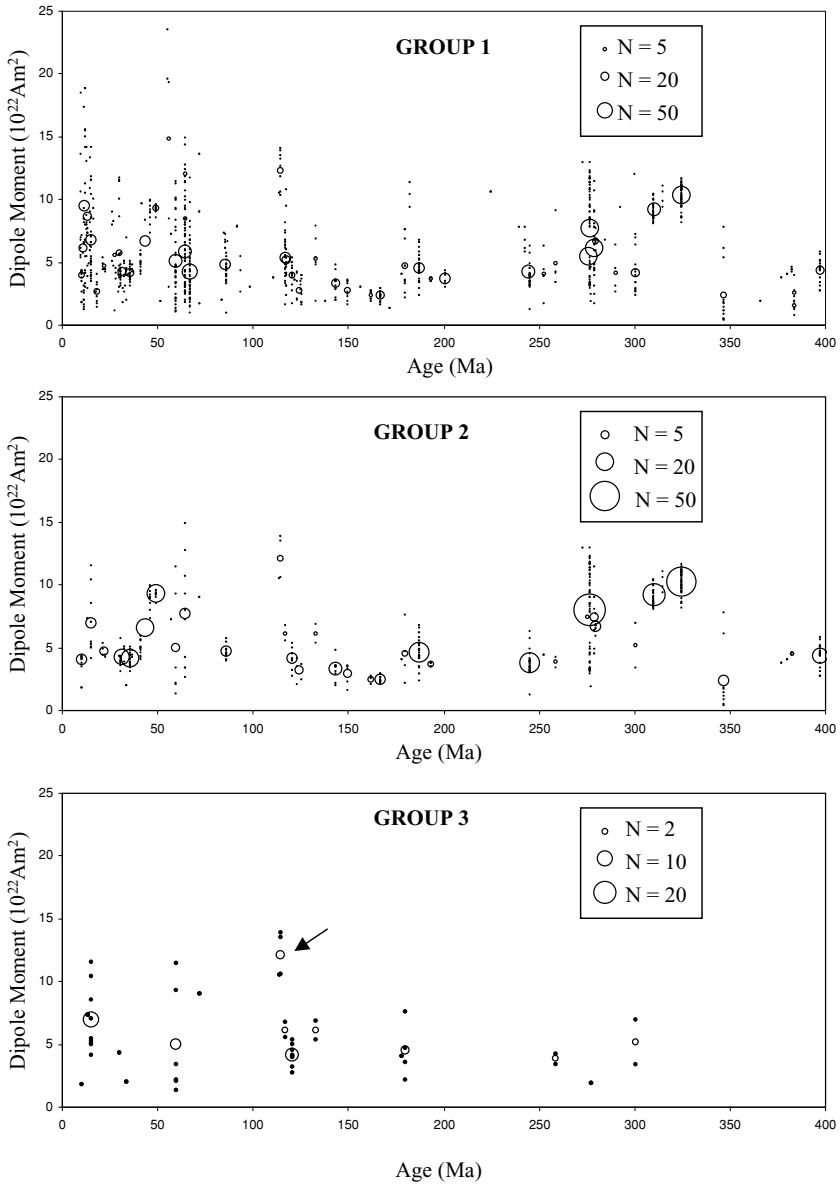

Figure 4. Plots of cooling unit (CU; black) and rock suite (RS; clear) data for the three groups of data. The size of each RS point is proportional to the amount of CU data it comprises and a representative scale is provided for each plot. The arrow on (c) draws attention to the RS produced by the study of Tarduno *et al.* (2001) which is discussed later.

values. Therefore, this ratio should not be used to compare the extent of dipole moment variation in different periods.

4.3 Reliability of the record

Selkin & Tauxe (2000) performed the most recent analysis of the global dipole moment record prior to this study using only estimates that were produced using the Thellier method with pTRM checks (T+). As stressed earlier, the use of pTRM checks does not guarantee reliability and, in the present study, internal consistency was also judged to be an important indicator of reliability. Hence, here for group 2 and 3 CU estimates, it was a requirement that, for each estimate, the standard deviation should not be more than 10 per cent of the mean. This is stricter than in Selkin & Tauxe (2000) where 25 per cent was chosen as the upper limit. Additionally, it should be noted that Selkin & Tauxe (2000) do not state that they rejected estimates comprised of only two determinations as we do, only that their criterion applies when estimates are derived from more than one determination.

The most relevant conclusion of Selkin & Tauxe (2000) to the present study was that average GPFI has remained constant in the period 300–0.3 Ma. This conclusion is clearly in disagreement with the findings of the present study based on the group 1 and 2 data sets and this warrants some investigation.

First, it is necessary to establish whether their conclusion remains valid when the updated database used in this study was analysed in the same way. From our group 1 data set, we used the same filtering steps as Selkin & Tauxe (2000) and applied a regression to the 158 CU estimates that remained (Fig. 9). An increasing trend through the 301–10 Ma period was observed to be significant at the 90 per cent (though not the 95 per cent) confidence level. Although the same time period is not characterized by a single trend in the

Downloaded from https://academic.oup.com/gji/article/152/2/392/653211 by guest on 04 February 2022

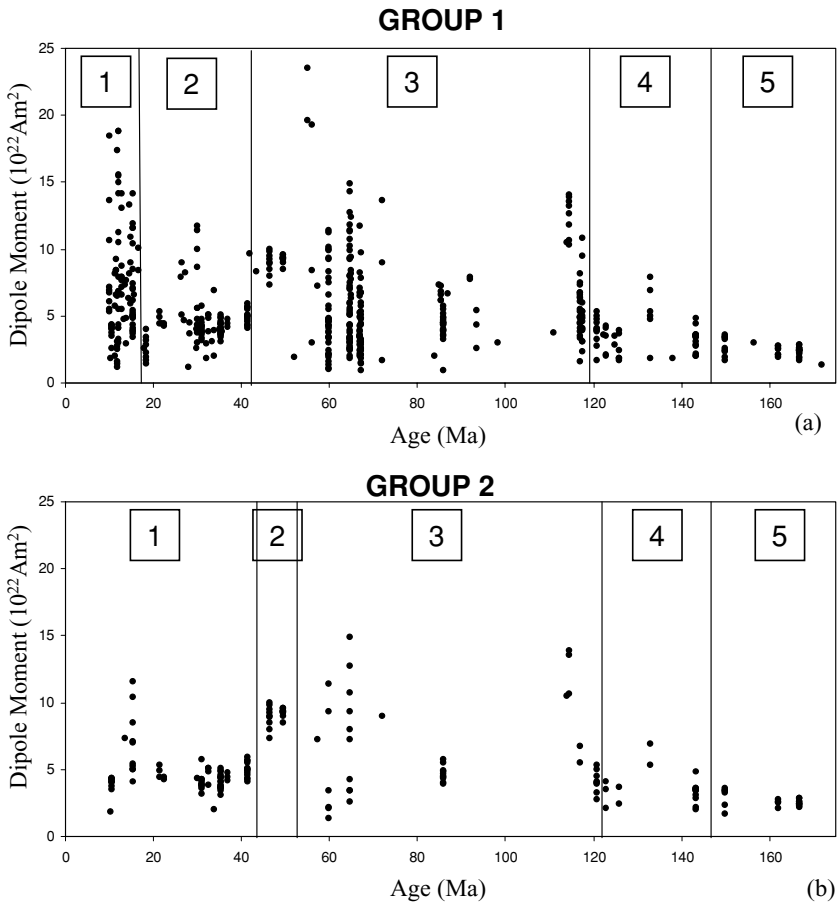

Figure 5. Plots of cooling unit data in the group 1 and 2 data sets from 172 to 10 Ma together with the locations of the segment partitions (vertical lines) derived from the analyses described in the text. The numbers of each of the corresponding segments is also given for clarity.

group 1 or 2 data sets of the present study (Figs 5a and b), such a result is not consistent with the Selkin & Tauxe (2000) conclusion that there has been no change in mean dipole moment during that period.

A further conclusion of Selkin & Tauxe (2000) was that any data set that contains a quantity of palaeointensity estimates not acquired using the T+ method is likely to be biased by such data. They reached this conclusion by comparing the CDFs of their data set with the unfiltered PINT97 database over the period 5–0 Ma and observing that they were significantly different. If such a conclusion were true then that could perhaps explain why the present study observed a variation in mean dipole moment over timescales of 10^7–10^8 Myr, while Selkin & Tauxe (2000) did not. In fact, this argument was partially addressed earlier when it was shown that the distributions of CU data in the group 1, 2 and 3 data sets were not significantly different from one another despite the discrepancy in perceived reliability between the average CU datum from each. This suggests that the presence of data not acquired using the T+ method, or even with poor self-consistency, does not impart a bias to the record. For completeness, the CDF of group 1 data was also compared with the CDF produced by the data filtered according to the criteria of Selkin and Tauxe (Fig. 3c). Once again, no significant difference was observed.

A further means of testing the possibility of biasing by unreliable data is to examine the quantity of potentially unreliable data in different parts of the record so that any systematic offsets can be recognized. To achieve this, the percentage of estimates in each segment obtained using methods other than T+ (Tables 2 and 3) was noted and plotted against the mean VDM of the segment (Fig. 10). No real relationship was observed for the group 1 data but some group 2 segments were observed to plot on a straight line with a negative slope (Fig. 10b). This relationship suggests that non-T+ data may indeed bias the mean towards low values and it is crucial to investigate this suggestion.

Four of the segments plotted in Fig. 10(b) comprised purely non-T+ data and these had a very wide range of associated mean dipole moment values, which is itself a strong argument against a single biasing agent. Segments 8 and 9 plotted well away from the trend line and will also not be considered here. The distributions for each of the other segments were independently subjected to ANOVA to determine whether there were any differences in the means of the T+ and non-T+ data comprising each of them. The results were sharply dichotomous: ANOVA rejected the null hypothesis of equal means for the groups within segments 1 and 4 at the 99 per cent significance level, whereas the same analysis of segments 3, 6 and 7 gave P values of greater than 0.9. The former result suggests that non-T+ and T+ data were behaving differently in these segments and consequently that these segments should be treated with caution. However, it should also be noted that there are only two T+ CU data, comprising one RS, in segment 4 and we cannot rule out coincidence as the reason for these having higher values.

Conversely, the results for segments 3, 6 and 7 strongly suggest that the means of these are unaffected by the relative proportions of

Downloaded from https://academic.oup.com/gji/article/152/2/392/653211 by guest on 04 February 2022

Table 2. Statistical description of individual segments defined in the text from the group 1 data set. μ_{age} and σ_{age} are the means and standard deviations of the age distribution for each segment. μ_{VDM} and σ_{VDM} are the overall means and standard deviations of the dipole moment distribution for each segment. in units of 10^{22} A m^2. N_{CU} and N_{RS} refer to the number of cooling unit estimates and the number of rock suite groups, respectively, in each segment and N_{RS}/N_{CU} is the ratio of these. Non-T+ gives the proportion of CU estimates in each segment that were not derived using the modified Thellier method with pTRM checks.

Segment	Age range	μ_{AGE} (Ma)	σ_{AGE} (Ma)	μ_{VDM}	σ_{VDM}	N_{CU}	N_{RS}	N_{RS}/N_{CU}	non T+
1	16.6–10 Ma	12.9	2.0	7.24	4.11	98	13	13%	70%
2	41.5–17.9 Ma	31.5	6.5	4.48	1.80	95	16	17%	71%
3	117.5–42 Ma	75.4	22.0	6.13	3.92	247	20	8%	65%
4	143.5–121 Ma	131.1	9.5	3.53	1.34	47	8	17%	57%
5	172–150 Ma	161.5	7.4	2.43	0.53	35	5	14%	97%
6	201–178 Ma	187.7	6.2	4.58	1.71	51	6	12%	67%
7	259–240 Ma	247.2	5.1	4.27	1.54	44	3	7%	89%
8	285–273 Ma	277.4	1.6	7.17	3.23	95	4	4%	97%
9	301–290 Ma	298.6	4.6	4.55	2.38	19	3	16%	5%
10	325–310 Ma	319.8	7.0	9.90	0.98	89	2	2%	100%
11	397.5–347 Ma	377.2	21.1	3.17	1.81	44	8	18%	100%

Table 3. Statistical description of individual segments defined in text from the group 2 data set. Headings as for Table 2.

Segment	Age range	μ_{AGE} (Ma)	σ_{AGE} (Ma)	μ_{VDM}	σ_{VDM}	N_{CU}	N_{RS}	N_{RS}/N_{CU}	non T+
1	41.5–10.3 Ma	28.5	10.9	4.68	1.47	75	9	12%	81%
2	49.5–46.5 Ma	48.1	1.5	9.08	0.64	19	2	11%	100%
3	121–57.5 Ma	87.1	24.4	6.25	3.54	42	8	19%	55%
4	143.5–123 Ma	137.0	8.8	3.55	1.21	18	3	17%	89%
5	167–150 Ma	160.9	7.6	2.61	0.51	20	6	30%	100%
6	193.5–178 Ma	187.0	3.8	4.44	1.21	33	4	12%	85%
7	259–245 Ma	246.2	3.8	3.76	0.88	30	3	10%	93%
8	280–273 Ma	277.1	1.3	7.75	3.22	74	4	5%	99%
9	301 Ma	301.0	—	5.15	2.47	2	1	50%	0%
10	325–310 Ma	319.5	7.1	9.85	0.96	83	2	2%	100%
11	397.5–347 Ma	379.5	22.9	3.70	1.82	29	5	17%	100%

T+ and non-T+ data and that their positions on the trend line are purely coincidental.

Therefore, there is no conclusive evidence to suggest that palaeointensity estimates produced using methods other than T+ have the potential to bias portions of the record towards low (or high) values. Such biasing, if it exists, may lead to difficulties in the interpretation of the earlier parts of the considered record where T+ data are very sparse or non-existent (Tables 2 and 3). Despite this, it is contested that nothing is gained by outright dismissal of non-T+ data at this stage. In fact, analysis and interpretation of such

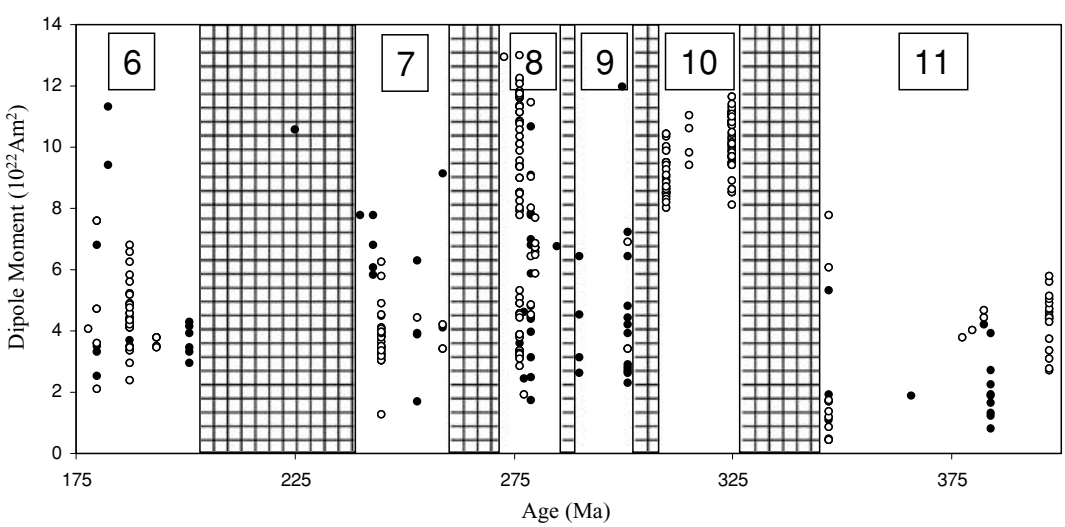

Figure 6. Plot of cooling unit data in the group 1 only (black) and group 2 (white) data sets from 397.5 to 178 Ma together with the locations of the segment partitions derived subjectively as explained in the text. Hatched areas represent 'dead' time periods in the records. The numbers of each of the corresponding segments is also given for clarity.

Downloaded from https://academic.oup.com/gji/article/152/2/392/653211 by guest on 04 February 2022

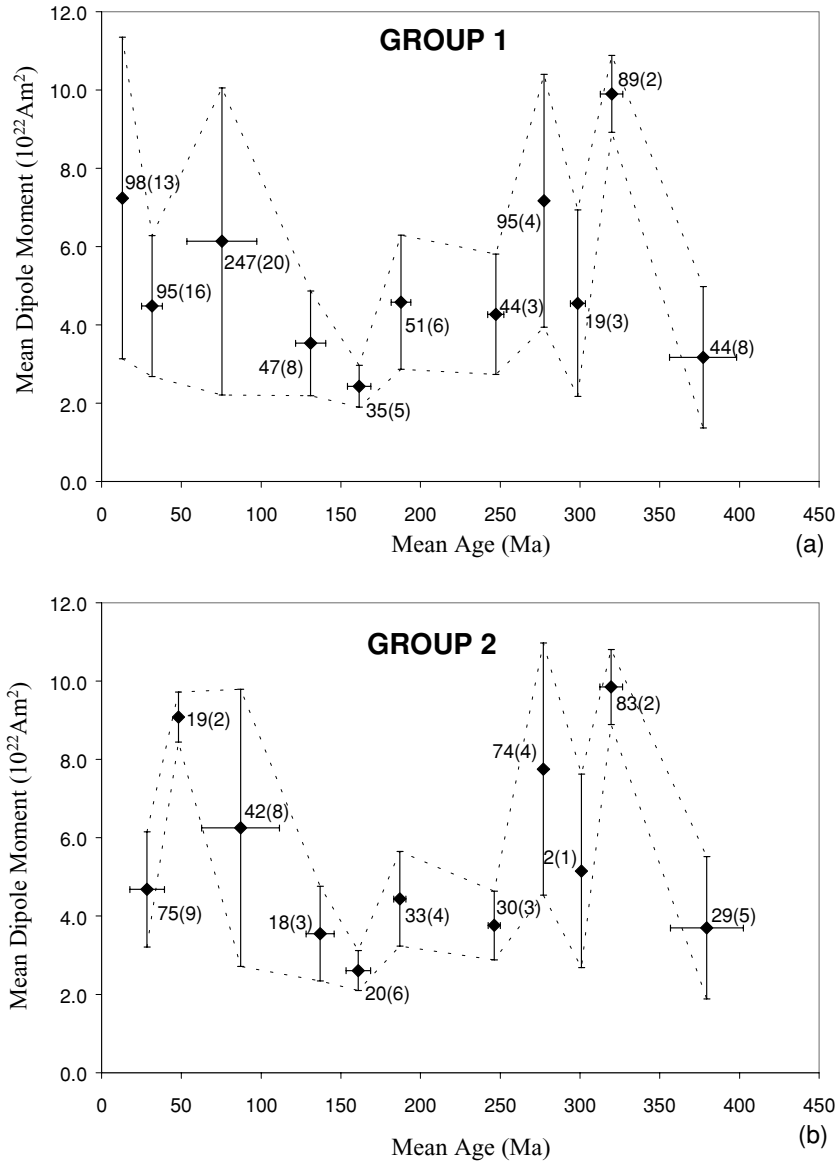

Figure 7. Plots of the mean ages and dipole moments of all segments from group 1 (a) and group 2 (b) data sets. The error bars indicate the standard deviation of each value and are representative of variation rather than uncertainty. The number of cooling unit estimates that comprise each segment and its corresponding number of rock suites (in brackets) are shown next to each segment mean. Dashed lines join the limits of segment means ± standard deviations to highlight the patterns of variation currently shown by the two data sets.

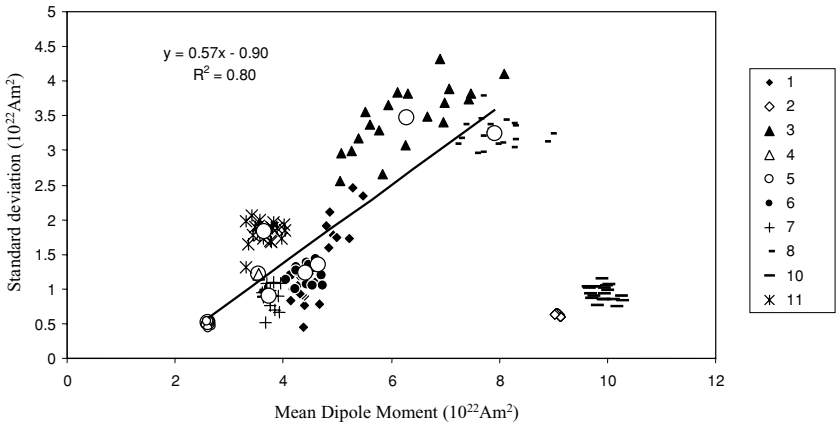

Figure 8. Plot of the mean dipole moment versus its standard deviation for 20 random samples of 20 cooling unit estimates from every segment except 9. Large open circles represent the means of each of the segment samples and the regression line and its equation are shown.

Downloaded from https://academic.oup.com/gji/article/152/2/392/653211 by guest on 04 February 2022

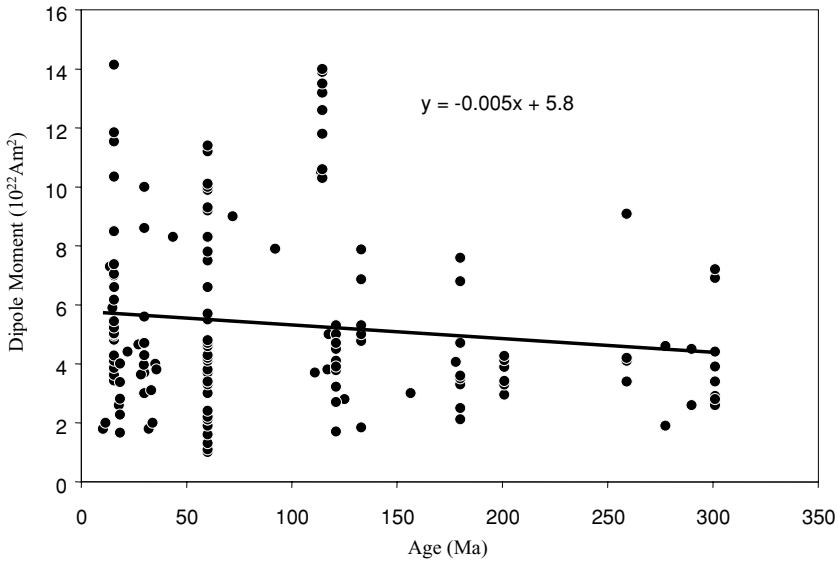

Figure 9. Plot of the distribution of data filtered according to the criteria of Selkin & Tauxe 2000), see text) from the group 1 data set. The line fit by regression analysis is shown together with its equation.

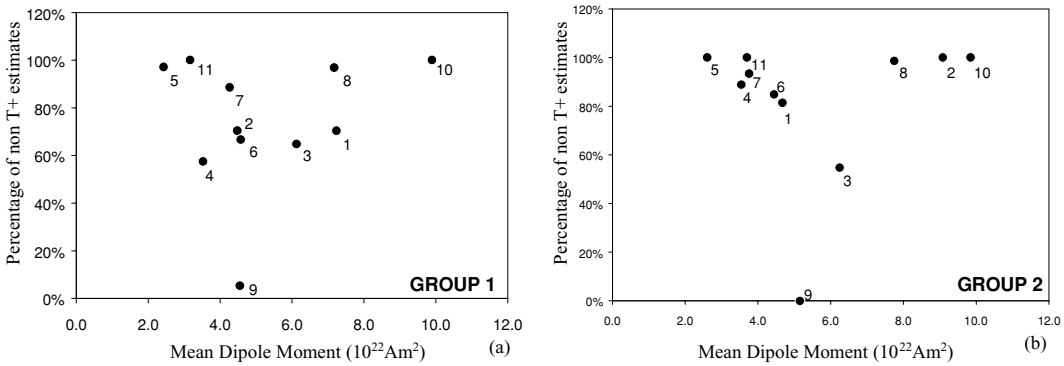

Figure 10. Plots for groups 1 and 2 showing the amount of cooling unit estimates in each segment that were derived not using the T+ method versus the mean dipole moment of that segment. Points are annotated with the segment number.

data will stimulate further research aimed at evaluating the reported observations.

4.4 Analysis of the group 3 data set

The group 3 data set was not partitioned in the same manner as groups 1 and 2 because of the low temporal density of CU data that comprise it. Nevertheless, it is perceived to contain the most reliable data points in the record and therefore some examination of its distribution through time is worthwhile. However, it must be noted that, whilst its dipole moment distribution is indistinguishable from the other groups, it does not exhibit the same trends through time, suggesting that aliasing effects may be present.

Fig. 4(c) suggests that there may have been an increasing trend of dipole moment through the time covered by the data. Nevertheless, the paucity of data prevents a regression being significant at any reasonable confidence level and this is still the case when the oldest data are omitted to exaggerate the trend. The regression analysis is based on the assumption that the response of each point (dipole moment in this case) is directly related to the value of the predictor (age) and so for a sparse data set such as this, secular variation acts to limit its effectiveness. Consequently, a different approach was adopted. The data set was partitioned at its temporal mid-point (150 Ma) and the two segments were compared using ANOVA. The result, as expected, rejected the null hypothesis of equal means at the 90 per cent confidence level, supporting the notion of long-term evolution of the dipole moment.

The only trend discernible (at the 95 per cent confidence limit) by regression analysis within the group 3 record is a decrease between 114.5 and 10 Ma. However, it is clear from the arrow in Fig. 4(c) that this is due almost entirely to four CU data with high dipole moments drawn from a single RS with an age of 114.5 Ma. This RS is evident as an outlier on the plot of group 3 data and, in fact, exerts a huge influence over both group 3 and 2 data. Such controlling factors will be discussed in the next section.

5 DISCUSSION OF THE STATISTICAL ANALYSIS

The analysis described above represents the most rigorous study of long-term dipole moment variation performed to date. The fact that, after over half a century of research in the field, such an analysis

Downloaded from https://academic.oup.com/gji/article/152/2/392/653211 by guest on 04 February 2022

can still be described as exploratory is indicative of the enormous difficulties associated with palaeointensity determination.

A primary aim of this study was to highlight areas of the record where data coverage was poor in terms of quality and/or quantity. Tables 2 and 3 provide a reference frame that can be used to target future palaeointensity studies to time periods when they would be most useful. Periods where data are few or absent are an obvious priority but the ratios of N_{RS}/N_{CU} and the proportion of non-T+ data, given for each segment, will also be useful in showing where new, high-quality data are most required. Features of the model presented in Section 6 will provide some additional impetus for such studies.

Fig. 7 shows unambiguously that the mean of dipole moment measurements in the group 1 and 2 data sets has varied on timescales of 10^7 and 10^8 yr. The analysis of the group 3 data performed in the previous section also strongly suggests a different distribution of data either side of an arbitrarily imposed division. Therefore, in contrast to Selkin & Tauxe (2000), it is evident that GPFI has varied over tens and hundreds of million years since at least the Carboniferous. Such long-term variation in geodynamo behaviour is very probably caused by changing conditions (most likely temperature and, to a lesser degree, thermal conductivity) in the lowermost mantle altering the boundary conditions at the CMB (Gubbins 1994; McFadden & Merrill 1995).

Fig. 8 indicates that there is a clear tendency for the mean and standard deviation of the dipole moment measurements in segments derived from the data to increase together regardless of the number of estimates or RSs within each segment (*cf.* Perrin & Shcherbakov 1997). Although the group 3 data set does not contain sufficient data to perform a similar analysis, the distribution of data in Fig. 4(c) suggests, qualitatively, that a similar pattern exists. Therefore, it can be stated with some confidence that when the mean GPFI is high, secular variation normally ensures that the lower limit of the possible GPFI range is very similar to that when the mean GPFI is low. Support for this concept also comes from analyses of relative palaeointensity variation through the Oligocene performed by Tauxe & Hartl (1997) and Constable *et al.* (1998) who concluded that the variability in measurements was proportional to the mean through the record. However, it is important to note that this relationship, approximated by the regression line shown in Fig. 8, does not intercept the origin as previously proposed (Perrin & Shcherbakov 1997) but cuts the x-axis at approximately 1.5×10^{22} A m^2.

5.1 Issues of reliability

Definite conclusions concerning the actual variations in GPFI through the time period studied are harder to generate and depend, to a degree, on the data set selected. This choice itself is a compromise depending on whether the 'safety in numbers' or 'safety in perceived quality' approach is preferred. In recent publications (e.g. Selkin & Tauxe 2000; Tarduno *et al.* 2001) the latter approach has certainly been the most popular. However, it is worthwhile to conduct a comparative discussion.

Again it is stressed that while the modified Thellier method incorporating pTRM checks is certainly the best palaeointensity method presently available, its results are not *guaranteed* to be accurate for the reasons given in Section 4.1. This is critically important because, by necessity, a high-quality data set has fewer data points and therefore more weight will be attached to any rogue points present within it. This problem is compounded in a small collection of palaeointensity estimates because of the inherent problem of secular variation. Tarduno *et al.* (2001) suggest the use of palaeomagnetic dipole moments to overcome this second problem. It is, of course, useful to know that the field is directionally averaged over 10^4–10^5 yr. However, the time-averaged direction of the field is always at one of the two geographic poles and therefore has a definite mean position. Conversely, when the intensity is undergoing a long-timescale ($>10^5$ yr) transition between one mean value and another, it is unclear what period of time constitutes a sufficient average. Furthermore, the additional problem of potential aliasing exists for overselected data sets and, therefore, any statistical analysis of long-term trends within these sets may well miss features that are characteristic of the true GPFI variation.

The validity of the 'safety in numbers' approach hinges on the question of whether the record can be *systematically* biased by unreliable data. The relationship suggested in Fig. 10(b) is intuitively pleasing: many palaeointensity experiments fail to give an accurate result because of the generation of ferromagnetic material within the sample during heating that shallows the NRM–TRM plot and produces an underestimate. Such an alteration would most likely be observed through pTRM-check discrepancies but may escape notice in an experiment that did not employ these. However, no systematic reduction of the mean by non-T+ estimates was observed in three of the five segments of data. Additionally, it should be noted that this is not the only form of possible alteration during a palaeointensity experiment. Kosterov & Prévot (1997) show an example of alteration during a Thellier experiment where the NRM falls away dramatically at the start of the experiment, resulting in an overestimate of the palaeointensity. This type of alteration would also probably be noticed if pTRM checks were employed but may otherwise escape attention. A crude form of support for the 'safety in numbers' approach can therefore be that, given sufficient data and in spite of the increased scatter, the mean should not be dramatically changed and long-term trends can still be accurately depicted. Furthermore, in the absence of any other cause of long-term variation we must conclude that actual changes in GPFI are forcing any observed variation (i.e. why should the data, if sufficient in quantity, be any worse on average in one part of the record than any other?)

The extreme arguments of either approach can obviously be dangerous. In particular, the arguments for the 'safety in numbers' policy rely on the assumption that, if biasing effects by groups of data (e.g. samples from a single lava succession where all flows altered in the same way) are present, there is a sufficient number of such groups acting in an opposite sense to cancel one another out. This identifies another advantage of using the rock suite method of grouping data in assessing reliability. For instance, segment 10 comprises 83 group 2 estimates but only two RSs. The RS method indicates that substantial new data from different sources are required for this time period to ensure not only that overrepresentation of short-term GPFI behaviour is avoided, but also that the segment is not biased by erroneous measurements.

The group 2 data set comprises data that not only satisfy rigorous palaeomagnetic and age criteria but also demonstrate high self-consistency (Section 4.1). Furthermore, there is no conclusive evidence to suggest that the data in this set bias the record towards low (or high) GPFI values. With this mind, the group 2 data set was selected here as the most appropriate basis for developing our geodynamic model (Section 6). The level of confidence that we can place in the earlier portion of this record is uncertain because of both the quality of the individual estimates and their scarcity through time. However, they remain the most reliable data available so the results are presented, but with an appropriate note of caution.

Downloaded from https://academic.oup.com/gji/article/152/2/392/653211 by guest on 04 February 2022

5.2 GPFI behaviour and its relationship with reversal frequency

Putting arguments concerning reliability to one side, it is worth discussing the consequences of the temporal variations in GPFI documented in the three data sets for our understanding of the geodynamo. Some numerical models of the geodynamo infer that GPFI is anticorrelated with reversal frequency (RF) (e.g. Glatzmaier *et al.* 1999). Sarson (2000) proposed fluctuations in the meridional flow within the core as a kinematic process causing reversals. In this model, the meridional flow acts to stop the dynamo operating in its oscillatory $\alpha\omega$ mode. It was argued that when the Glatzmaier–Roberts dynamo was subject to high polar heat flux as in Glatzmaier *et al.* (1999) and meridional flow (and hence poloidal field) was strong, the field was also less prone to reversals and excursions. If this mechanism were active in the geodynamo, the mean GPFI and the reversal frequency would be anticorrelated in the palaeomagnetic record.

The notion of anticorrelated reversal frequency and GPFI was supported by the results of Thellier analyses on titanomagnetite inclusions in the Rajmahal Traps performed by Tarduno *et al.* (2001). This produced the RS with a high dipole moment at 114.5 Ma that was mentioned earlier as having a great deal of influence on the group 2 and 3 records. It is clearly evident that, in the absence of this result, the group 3 data would show a very gradual and continuous increase in dipole moment (Fig. 4c) and that the configuration of the segment partitions in the group 2 data would be quite dramatically altered (Fig. 5b). The CU estimates presented by Tarduno *et al.* (2001) were produced by applying the reliable T+ method to single plagioclase crystals to reduce the possibility of thermally induced alteration. The original nine CU estimates also constitute a palaeomagnetic dipole moment, although the four that pass the self-consistency criterion necessary to enter the group 2 and 3 data sets probably do not. In spite of the high quality of the data, this single RS cannot be sufficient to confirm anticorrelation.

In contrast to the results of Tarduno *et al.* (2001), many other studies concerning palaeointensity data acquisition and analysis (e.g. Prévot & Perrin 1992; Thomas *et al.* 1997, 1998, 2000; Selkin & Tauxe 2000) have favoured a decoupling of processes controlling the mean GPFI and reversal frequency, but have not attempted to explain how this would be possible. One alternative to the kinematic process outlined by Sarson (2000) is that the geomagnetic field undergoes excursions and reversals when the geodynamo collapses into a weak-field state (Zhang & Gubbins 2000a; Zhang & Gubbins 2000b). The reversal frequency would then most likely be controlled either by the susceptibility of the geodynamo to collapse or the average length of time the geodynamo spent in a weak-field state once it had collapsed. Both factors would dictate the likelihood of the field diffusing out of the inner core and hence the geomagnetic field adopting a different polarity once the strong-field state was re-established. The extent to which these factors could be decoupled from the capacity of the geodynamo to generate poloidal field in its strong-field state is not currently known. Gubbins & Zhang (2000) have suggested that the process of polarity reversal may be controlled by lateral variations of heat flux *within* the CMB region. As discussed earlier, GPFI changes are more likely to be controlled by total heat flux *across* the CMB region. This presents an intuitive explanation for how GPFI and RF could be decoupled: GPFI responds to absolute changes in net heat flux away from the core while RF is more sensitive to relative changes in the spatial pattern of this heat flux.

Using the results of the present study, the RF-GPFI issue is best addressed by focusing on the period of time between the Middle Jurassic and 10 Ma when the timing of polarity intervals is well known. Two opposing interpretations of RF behaviour have been proposed for this period. McFadden & Merrill (1997) concluded that RF decreased continuously from ~4.5 Myr^{-1} to zero in the period 160–118 Ma, where it remained until 83 Ma, and rose more gradually to ~ 4.5 Myr^{-1} from 83 Ma to recent times. Gallet & Hulot (1997), on the other hand, suggested that RF exhibited stationary behaviour between 160 and 130 Ma and from 25 Ma to the present, with a long period of non-stationarity between 130 and 25 Ma. McFadden & Merrill (2000) have demonstrated, statistically, that there is neither a requirement nor support in the data for discontinuities in the RF at 130 and 25 Ma, rendering the Gallet & Hulot (1997) interpretation untenable. It is noted, however, that the statistical analysis of Constable (2000) could not discount either interpretation.

When the segments derived for either group 1 or group 2 data are used as a description of mean GPFI behaviour, punctuated increases separated by periods of stasis are evident between the Middle Jurassic and Eocene (~ 45 Ma). This is clearly unrelated to RF variation during this time (decrease followed by stasis, followed by an increase), suggesting that the two parameters are decoupled. The method of segmenting the GPFI record used here was selected so that the data themselves, rather than an arbitrarily imposed time factor, determine the location of the partitions. Some of the generated segments (particularly the crucial segment 3) are rather large, indicating that the present database can only provide reliable information on GPFI variations at a low resolution. Therefore, the method is invaluable in determining what we can tell concerning long-term GPFI variations (e.g. Fig. 7b). Nevertheless, such a segmented record, containing divisions up to 63 Myr apart, will inevitably smooth out subtle changes in GPFI that may be important in ascertaining the existence and nature of a link with RF. With this in mind, group 2 data with ages less than 170 Myr were grouped into 10 Myr bins in order to improve the resolution in this period. As expected, the observed variation in the segment means is rather noisy (Fig. 11) and therefore only limited recognition of genuine GPFI variation is possible. However, when this plot is compared with one showing the number of polarity reversals in the same 10 Myr intervals (plotted using a reverse scale in Fig. 11) it is not possible to rule out an anticorrelation of RF and GPFI. There is obvious disagreement in the 80–90 Ma bin and minor disagreement elsewhere. However, the two highest values of mean GPFI correspond to

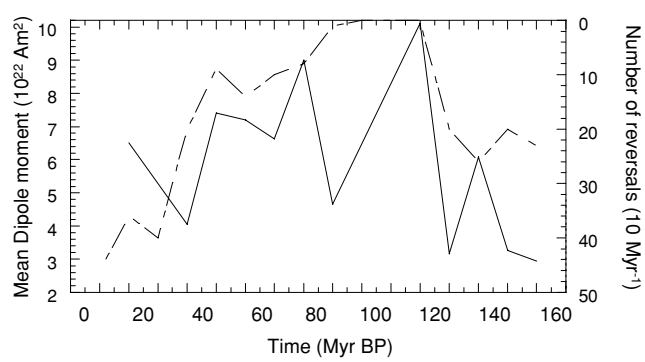

Figure 11. Plots of mean dipole moment (solid line) for group 2 data and number of polarity reversals (dashed line) in 10 Myr bins for the period 170–10 Ma. Note the reversed scale on the right-hand side.

Downloaded from https://academic.oup.com/gji/article/152/2/392/653211 by guest on 04 February 2022

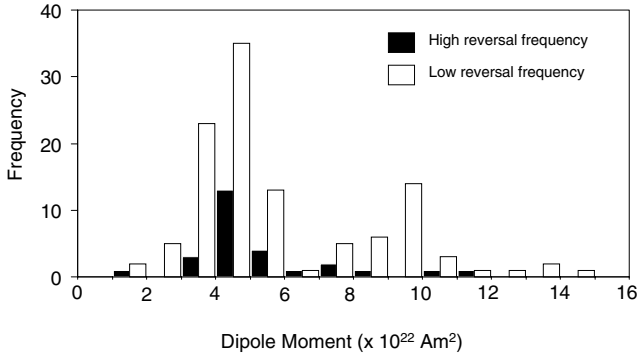

Figure 12. Histogram showing the distribution of group 2 dipole moment data from times of high reversal frequency (10–30 Ma) and low reversal frequency (123–30 Ma).

segments containing a low number (<10) of polarity reversals and the three lowest segment means correspond to a high number (∼20) of reversals.

Selkin & Tauxe (2000) discounted any relationship between RF and GPFI by showing that the distribution of their dipole moment data for times when RF was high (30–0.3 Ma) was indistinguishable from that when the RF was low (124–30 Ma). The same analysis was performed here using the group 2 data set. In this case, the distribution of data drawn from the period of low RF (Fig. 12) appears to have a secondary peak at higher values (8–11 $\times$ 10^{22} A m^2) that is not present in the data distribution from the period of high RF. This indicates that GPFI may have behaved differently during periods of differing mean RF, having a frequent tendency to be high during periods of low RF. However, a simple anticorrelation is not the only explanation that could account for the distribution shown in Fig. 12. Unfortunately, the paucity of absolute palaeointensity data precludes a more rigorous analysis at this stage. The record of GPFI is subject to significant, most likely, random fluctuations when viewed at a resolution sufficiently high to allow direct comparison with RF. Therefore, in conclusion, the density of reliable palaeointensity estimates is presently insufficient to confirm an anticorrelation of GPFI and RF. This highlights the need to supplement the Middle Jurassic–Late Tertiary period (particularly at times within the CNS, Fig. 14, below) with more high-quality palaeointensity data.

Elsewhere in the record, a major transition in GPFI behaviour occurs coincident with the PCRS (∼320–260 Ma) as seen in Fig. 7(b). After increasing rapidly prior to the PCRS, GPFI appears to decrease during the superchron itself. A sharp rise in GPFI at the time of superchron *onset*, also suggested for the CNS, constitutes evidence for a common cause of major perturbations in the two geomagnetic parameters. However, the observation that GPFI underwent large changes during a time of constant, zero RF provides evidence for decoupling during the *bulk* of the superchron, suggesting that the stability in the processes controlling RF is not reflected in the processes controlling GPFI variation. The low density of rock suites covering the PCRS must, of course, be regarded as a limiting factor in this discussion. However, it is emphasized that, assuming a quasi-symmetrical variation in RF between the superchrons, only slight modifications to the positions of the segment means in Fig. 7(b) would be needed to obtain a strong anticorrelation. It is also worth noting that a study of relative palaeointensity in Oligocene sediments (Tauxe & Hartl 1997) provides some support for anticorrelated GPFI and RF.

Figs 7(b), 11 and 12 give no support to the suggestion, made by Loper & McCartney (1986), that the geodynamo becomes more

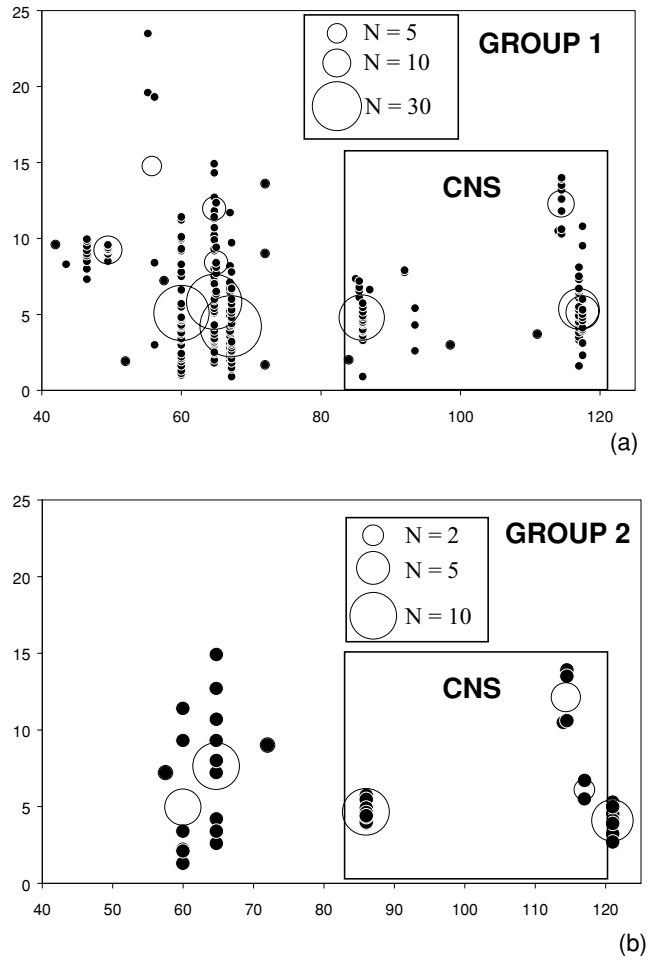

Figure 13. Plots of cooling unit (black) and rock suite (white) distributions for segment 3 from groups 1 and 2 data sets. Representative scales for the RS points are given and the boxed areas represent estimates taken from times during the Cretaceous normal superchron.

erratic when in a vigorously convecting mode, leading to positive correlation of GPFI and RF. Therefore, the present palaeointensity database is sufficiently detailed to discount this theory and allow future studies to focus on the remaining possibilities: do superchrons represent high-power DC states of the geodynamo? Are RF and GPFI decoupled? Or, does a more complex relationship exist?

The extent to which PSV changes during superchrons is an issue of current interest. A recent palaeomagnetic study of sediments in SE France suggested that PSV during the PCRS was similar to present-day variation (Kruiver *et al.* 2000). The present global dipole moment record suggests that this was not the case for the CNS. Fig. 13 shows that for segment 3, in both group 1 and 2 data sets, the distributions of CU data from times within the CNS are clearly different from those for times outside the CNS. In particular, there is a virtual absence of low (<3 $\times$ 10^{22} A m^2) estimates in the group 2 CNS data set and a reduced variance for both group 1 and 2 data for times within the CNS relative to times outside. The cumulative distribution functions for these data (Fig. 14) confirm these observations. However, caution should be exercised since the group 2 RS data, particularly within the CNS, are few and confined to the extremities of the superchron. Nevertheless, the results are intuitive because fluctuations in all geomagnetic parameters are expected to be reduced during long, stable periods of constant polarity. This idea recently

Downloaded from https://academic.oup.com/gji/article/152/2/392/653211 by guest on 04 February 2022

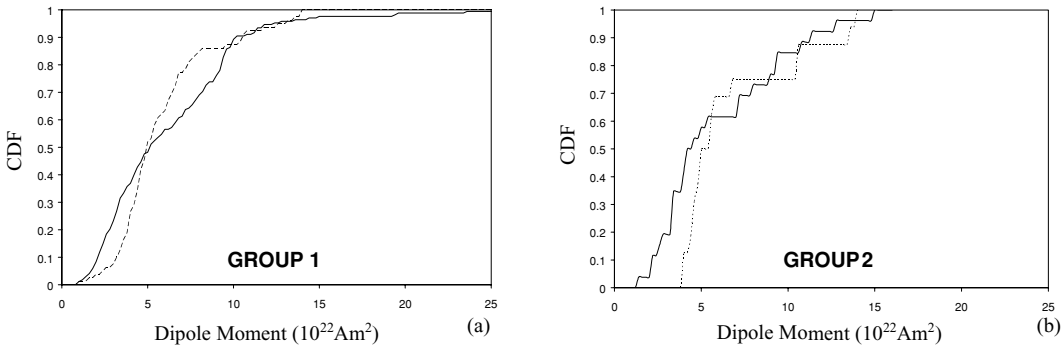

Figure 14. Cumulative distribution functions for data from segment 3 of groups 1 and 2 comparing data from outside (solid line) and inside (dashed line) of the times of the Cretaceous normal superchron.

received some support from a detailed palaeomagnetic study of two sedimentary sequences spanning the period 85–89.5 Ma from central Italy (Cronin *et al.* 2001). The two stratigraphically overlapping sequences, separated by a distance of 20 km, displayed good correlations in both directional and relative palaeointensity variation. Together they suggested that PSV expressed in both direction and intensity was reduced during this period relative to times when the geomagnetic field undergoes frequent polarity reversals. Unfortunately, before reduced PSV during the CNS can be confirmed by absolute palaeointensity measurements, the period must be supplemented with further RS data in order to dismiss the possibility of this observation being explained by rogue transitional data or over-representation of short spells of PSV.

The trends in GPFI through time, identified in the group 2 data, are listed below in stratigraphic order and illustrated in Figs 4(b) and 7(b). The reliability of each can be assessed easily using the data given in Table 3 applied to the pertinent segment(s). Prior to 50 Ma, the broad features indicated by the group 1 data are almost identical to those given here.

(1) GPFI was low ($<5 \times 10^{22}$ A m^2) during the Devonian and earliest Carboniferous.

(2) A sharp increase in GPFI occurred between 350 and 325 Ma, followed by a more gradual decrease from 325 Ma to at least around 250 Ma, but possibly the Early Jurassic (the scarcity of data prevents greater accuracy).

(3) GPFI was at a minimum ($<3.5 \times 10^{22}$ A m^2) in the Middle Jurassic ($\sim$170 Ma).

(4) The mean GPFI rose from the Middle Jurassic to the Eocene ($\sim$170–50 Ma), with the suggestion (unconfirmed owing to data paucity) of a plateau from 120 to 60 Ma.

(5) Through the Eocene (50–40 Ma), GPFI fell to a mean value of $\sim 4.5 \times 10^{22}$ A m^2, which was maintained until at least 10 Ma.

The final two points are based upon the segments derived from the ANOVA/regression analyses described earlier and consequently are rather sensitive to the age distribution of individual CU estimates. It is stressed that these features are not presented as a final description of mean GPFI during the period concerned. The dangers of overinterpretation of what is still, essentially, a limited data set are clear. Nevertheless, it does represent the best model for the current group 2 data set and will be useful in allowing future palaeointensity estimates to be compared with existing data from the same segments.

The limited analysis that was performed on the group 3 data set indicated that it was subject to long-timescale changes. However, the data set is so sparse that the only real inference regarding the nature of this change is that mean GPFI appears to have an overall increasing trend throughout the entire period 300–10 Ma. Whilst opposing the conclusion of Selkin & Tauxe (2000), this is not entirely consistent with the group 1 and 2 distributions, which suggest that GPFI was relatively high in the Early Permian decreasing towards the Permo-Triassic boundary. However, such comparisons are not very meaningful because there is a danger of PSV biasing and/or aliasing in the group 3 record. The present study (e.g. Figs 4–7; Tables 2 and 3) highlights the need for rigorous methodology in future palaeointensity studies. Work should concentrate on filling the well-defined gaps in the database, using suitable rock types and palaeointensity techniques to produce results that qualify for group 3 status. Undoubtedly the microwave Thellier technique, pioneered at Liverpool, will become increasingly important in palaeointensity work. This is particularly clear given the recent successes achieved on ancient lavas using this technique (e.g. Hill *et al.* 2002). Targeted future studies will, hopefully, provide sufficient data to enable a similar form of segmentation on a group 3 data set to that used on groups 1 and 2 here.

6 RELATIONSHIP BETWEEN PALAEOINTENSITY AND GLOBAL GEODYNAMICS

6.1 The generic model

The following chain of events is proposed to explain the generic link between GPFI variation and geodynamic evolution.

(1) Large-scale subduction of cool oceanic crust, resulting from intense plate tectonic activity at the Earth's surface, is followed by accumulation of subducted material at the 660 km thermal boundary layer (e.g. Honda *et al.* 1993).

(2) The accumulated material eventually becomes gravitationally unstable, passes through the 660 km transition into the lower mantle and avalanches catastrophically down to the CMB region. Such destabilization events have been produced by numerical models of mantle convection (e.g. Tackley *et al.* 1993; Yuen *et al.* 1994; Davies 1995) where material descends rapidly through the lower mantle and spreads out to form a thick layer over the CMB where it can reside for a period in excess of 50 Myr (Yuen *et al.* 1994). Temperature differences in excess of 1000 K exist, presenting favourable conditions for increased convection. The introduction of large quantities of cool material into the lower mantle will result in counter-flow of material moving up elsewhere, since the mantle is expected to be incompressible (Trompert & Hansen 1998). This counter-flow is assumed to involve the whole of the lower mantle.

Downloaded from https://academic.oup.com/gji/article/152/2/392/653211 by guest on 04 February 2022

(3) The *thermal* signature of the descending material may not be transferred to the CMB for some considerable time. Ricard *et al.* (1993) estimate it takes 50 Myr for a descending slab to register a thermal effect at the CMB. However, the introduction of material into the lower mantle would enhance convection everywhere so that heat flux across the CMB would be increased almost instantaneously and would be proportional to the volume of material introduced. This process is termed forced or induced convection (e.g. Anderson 1998).

(4) Consequently, heat flux out of the core increases, which in turn, causes the outer core to convect more vigorously, thereby increasing the total geomagnetic field intensity (Buffet *et al.* 1996; Buffet 2000).

6.2 Testing the geodynamic model: correlations between GPFI variation and the evolution of Pangaea

The model in Section 6.1 suggests that palaeointensity variations (represented by GPFI) should be a directly measurable effect of geodynamic evolution via a defined chain of events. Supercontinents are transient surface expressions of geodynamic evolution, existing periodically throughout geological time (Yale & Carpenter 1998). We propose that their evolutionary cycle can be documented by long-term trends in the palaeointensity record. According to our generic model, prolonged episodes of *minimal subduction* (when supercontinents were assembled) would be documented by periods of *low palaeointensity*. Conversely, *increased subduction* (supercontinents assembling or dispersing), would result in an *increasing or high palaeointensity*.

The statistical analysis of Section 4 demonstrates that GPFI varies on timescales of 10^7–10^8 yr because of changing conditions in the lowermost mantle. Consequently, measurements of dipole moment must be treated collectively so that a time-averaged record of GPFI variation is obtained and the longer-timescale variation is isolated. The age range (400–10 Ma) covered by the GFPI record analysed in Section 4 provides an ideal opportunity to test our proposed model since it corresponds to a major part of the evolutionary cycle of the supercontinent Pangaea.

The basic pattern of mean GPFI variation (Fig. 7b) indicates that there are key stages in the evolution of the GPFI record since the Devonian. The following analysis attempts to provide a geodynamic interpretation for each stage, using the logic described in Section 6.1 and other geoscientific evidence. The Pangaea model, illustrated in Fig. 15, is a first-order interpretation based on the long-term GPFI variations illustrated in Fig. 7(b) and further informed by the GPFI behaviour witnessed in the segment analysis (Figs 4 and 5). Inevitably, it contains some ambiguities and these are discussed in Section 7.

Stage 1: 400–350 Ma, low GPFI (Fig. 15a)

Subduction of Iapetan crust was prevalent for approximately 50 Myr prior to the *ca.* 425 Ma collision of Baltica (moving rapidly at $\sim$10 cm yr^{-1}) and Laurentia (stationary) (Eide & Torsvik 1996). By 400 Ma, a considerable volume of subducted crust had collected at the 660 km transition. Throughout the period 400–350 Ma, the newly formed Baltica–Laurentia crust moved rapidly southwards and the European massifs and Gondwana moved northwards towards it. Subduction therefore continued, providing further source material for the cold reservoir accumulating at 660 km. We propose that the upper and lower mantle were convecting separately during this time because the accumulated material did not have sufficient gravitational instability to penetrate 660 km. Therefore, the lower mantle could only have lost heat by conduction through the 660 km boundary and would have become very warm (Davies 1998) resulting in low heat flux across the CMB and a consequently low GPFI (Fig. 15a).

Stage 2: 350–250 Ma, rapid increase in GPFI, followed by a less-rapid decrease (Fig. 15b)

The extremely sharp rise in GPFI evident in the period 350–325 Ma implies that heat flux across the CMB increased rapidly during this time. We propose that this resulted from large quantities of cool material being introduced into the lower mantle, via a catastrophic episode of avalanching when the accumulated material eventually became gravitationally unstable and overcame the resistance of the phase change boundary at 660 km. Such destabilization events have been produced by numerical models of mantle convection (e.g. Tackley *et al.* 1993) and may have, in this case, been triggered by slab delamination after continent–continent collision resulting from the continued accretion of Pangaea (Eide & Torsvik 1996). During the period 325–250 Ma, GPFI decreased suggesting that the heat flux across the CMB also decreased. This presumably reflects a stage of restabilization subsequent to the avalanching event with the mantle becoming progressively warmer. We suggest two reasons for this warming. First, the majority (but not all) of Pangaea was likely to be in place by 320–300 Ma and therefore the bulk of subduction had ceased (e.g. Muttoni *et al.* 1996) reducing the availability of cold, relic lithospheric material for introduction into the lower mantle. Secondly, the insulating effect (e.g. Anderson 1982) of the supercontinent would have been a considerable factor in gradually increasing the (already high) ambient lower-mantle temperatures.

Stage 3: 250–175 Ma, generally low GPFI (Fig. 15c)

During this stage, the GPFI was generally low (Fig. 7b), being characterized by part of the feature known as the Mesozoic dipole low (Prévot *et al.* 1990). The absence of significant GPFI variation reflects the low heat flow across the CMB and implies a period of relative geodynamic quiescence during the period when the supercontinent was assembled. The final amalgamation and initial rifting of Pangaea is believed to have almost overlapped, with a singularity (total supercontinent) thought to have occurred at 230 $\pm$ 5 Ma (Veevers 1989). Initial rifting across Pangaea had already begun (Veevers 1989) though the first appearance of sea floor would not have occurred until stage 4, below. The insulating effect of the amalgamated supercontinent would therefore have been at its maximum during this stage, as witnessed by the position of the geoid high (Anderson 1982) suggesting that the mantle was at its hottest during these times, which is consistent with our model. The lack of subduction and subsequent avalanching allowed the upper and lower mantle to convect separately.

Stage 4: 175–10 Ma, gradual increase in GPFI, followed by a decrease (Fig. 15d)

The early part of this period (175–120 Ma) was characterized by a very gradual, but definite, increase in GPFI. This is interpreted as reflecting the increase in CMB heat flux in response to a steady introduction of cold, subducted material into the lower mantle following the resumption of widespread subduction in the Middle Jurassic as the dispersal of Pangaea gathered momentum. The negative

Downloaded from https://academic.oup.com/gji/article/152/2/392/653211 by guest on 04 February 2022

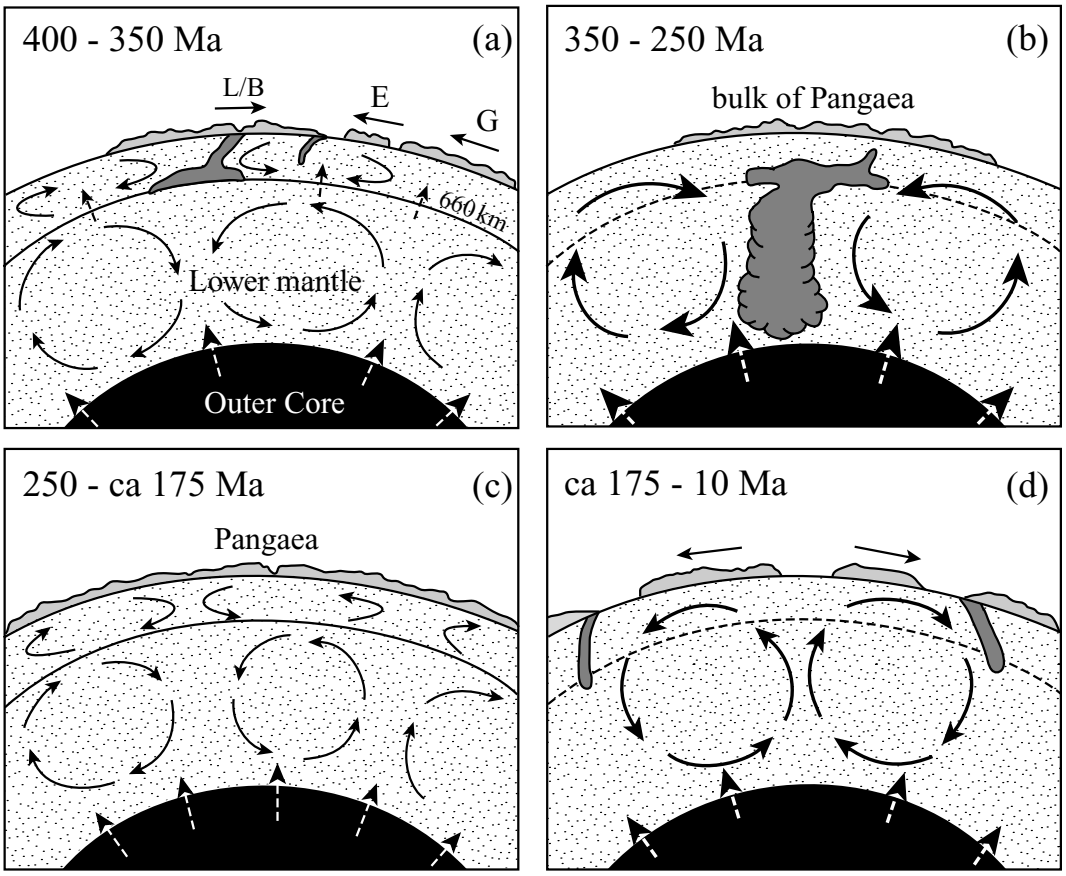

Figure 15. Cartoon to illustrate the four broad stages in the evolution of Pangaea from 400 to 10 Ma, as defined by the trends in the geomagnetic poloidal field intensity record. (a) 400–350 Ma: GPFI low and steady, (b) 350–250 Ma: initial rapid increase in GPFI, followed by a more gradual decrease, (c) 250–175 Ma: GPFI low and stable, (d) 175–10 Ma: increase in GPFI to a poorly constrained peak, followed by a decrease to a low at ∼ 40 Ma and subsequent stasis.

buoyancy of the descending slabs would now be greater than in stage 1 because the upper mantle was hotter and therefore less viscous. Also, oceanic lithosphere had more time to cool at the surface than in stage 1 when higher plate velocities were observed (Eide & Torsvik 1996). We propose that the resulting increased momentum of the subducted slabs during the initial stages of Pangaea dispersal would have allowed them to penetrate the 660 km transition more readily than the period prior to the formation of the supercontinent (stage 1). During the subsequent period, from 120 to *ca.* 10 Ma, tectonic evidence clearly shows that subduction was prevalent as Pangaea dispersal continued but, initially, (120–60 Ma) GPFI appears to show no evolution (segment 3). However, caution must be applied since this segment is heavily influenced by a single rock suite at its margin and characterized by a lack of data coverage in its bulk and, therefore it is possible that GPFI actually continued to rise throughout this time. The increase, followed by decrease in GPFI, either side of a peak at ∼50 Ma possibly documents a major avalanching episode associated with a significant tectonic event during the latter stages of Pangaea dispersal (see Section 7 for a discussion). The subsequent restabilization of the mantle appeared to continue until at least 10 Ma, after which GPFI began to increase toward its current value.

7 DISCUSSION OF THE GEODYNAMIC MODEL

The model proposed and tested here to explain the observed GPFI variations since the Early Devonian is a first-order model adopting the view that subduction, rather than plume activity, is the dominant force in driving mantle convection (e.g. Anderson 1994, 1998; Heller *et al.* 1996; Sheth 1999; Dalziel *et al.* 2000). It relies on the assumption that GPFI is proportional to the total heat flux across the CMB. This is supported by the observation that the total geomagnetic field strength (poloidal + toroidal) is proportional to the vigour of outer core convection (Buffet 2000), which is itself related to the total heat flux across the CMB (Buffet *et al.* 1996). Loper & McCartney (1986) also note that cooling of the core powers the geodynamo. The model requires the following fundamental features, each of which has support from independent sources:

- the occurrence of catastrophic avalanching of material into, and through, the lower mantle;
- the subsequent counter-flow of material involving the entire mantle; and
- the ability of the mantle convection regime to change between being layered and whole.

The existence of seismically identified cold anomalies at the CMB below the Pacific rim are spatially correlated with Pacific subduction zones (Yuen *et al.* 1994; Wen & Anderson 1995; Lay *et al.* 1998) and have been interpreted as remnants of oceanic lithosphere subducted during the past 120 Myr. The detached appearance of these masses and their large temperature contrast with surrounding mantle material (>1000 K) suggest that their presence at the CMB is caused by catastrophic flushing or frequent avalanching following periods of lithosphere accumulation at the 660 km transition (Honda

Downloaded from https://academic.oup.com/gji/article/152/2/392/653211 by guest on 04 February 2022

et al. 1993; Tackley *et al.* 1993; Yuen *et al.* 1994). It is logical that a counter-flow should exist in response to the catastrophic introduction of a significant mass into the lower mantle, given that the mantle is expected to be incompressible. Furthermore, 3-D models of partially layered mantle have shown that slab penetration into the lower mantle is expected to result in some form of counter-flow (Tackley 2000). The two avalanching events proposed in our model would require an associated counter-flow involving the entire mantle. Support for this comes from Tatsumi *et al.* (2000) who observed that hotspot activity was suspected to be widespread in the Mid-Carboniferous, suggesting that one or more large plumes formed as a counter-flow to an avalanching event. Larson & Kincaid (1996) also proposed counter-flow following slab penetration of the 660 km layer as a cause of the upward advection of the layer and subsequent plume activity later in geological time.

Davies (1995) presented a numerical model indicating that layered mantle convection followed by catastrophic avalanching may have existed at ∼ 1 Ga when the Earth was warmer. It is proposed that a similar scenario was active during stage 1 of our model. Prévot *et al.* (2000) regard TPW stability to indicate the existence of layered mantle convection, whereas a TPW peak documents a period of avalanching, mantle reorganization and counter-flow in the form of plumes and is supportive of single-layer convection. This view is shared by Eide & Torsvik (1996) and independent evidence from Machatel & Weber (1991) and Brunet & Machatel (1998).

The model proposed here does not specifically require lateral variations in CMB heat flux, which nonetheless, are thought to exist (e.g. Lay *et al.* 1998; Russell *et al.* 1998). However, if GPFI was highly sensitive to lateral variations, then, as plate reorganizations occurred, it would be expected to vary substantially and frequently over shorter time periods than those evident in the present record.

The proposed model is certain to contain oversimplifications owing to the limitations of the data themselves and the subsequent statistical analysis. It is therefore not appropriate to overinterpret the features seen, although outlining potential implications is important in the context of constraining future work. One key example is in the period 120–60 Ma. This period is crucial in geomagnetic terms because it contains the CNS, and geodynamic terms because it contains one of the most intensive periods of plume-related basaltic activity in the geological record (e.g. Larson 1991). Significant plume activity, or any other form of mantle mass redistribution, would intuitively be expected to feature in the record of true polar wander. Courtillot & Besse (1987) regard the emission of plumes from a thickened CMB to be a controlling feature in determining TPW and RF variation. Besse & Courtillot (1991) concluded that TPW has been episodic since 200 Ma, with the main period of low TPW (between 180 and 110 Ma) being coincident with a decrease in reversal frequency into the CNS. A period of fast TPW, from 110 to 50 Ma correlates with increasing reversal frequencies. Prévot *et al.* (2000) have suggested that a TPW peak occurred at ∼110 Ma in response to a major avalanching and mantle reorganization event. They link the TPW high to the occurrence of plume hyperactivity at the surface. The existence of this '110 Ma event' is disputed by Tarduno *et al.* (2001) who regard it as an artefact of Atlantic hotspot motion. They argue that the method of TPW calculation used by Prévot *et al.* (2000) is invalid because the assumption that hotspots are stationary in a convecting mantle is not true, as demonstrated in independent studies (e.g. Cande *et al.* 1995; Steinberger & O'Connell 1998; Steinberger 2000; DiVenere & Kent 1999). Tarduno *et al.* (2001) conclude that the position of Earth's spin axis has not altered by more than ∼5° over the past 130 Myr and Tarduno & Smirnov (2002) find no palaeomagnetic data to support the dramatic rotation of the entire Earth required by the Prévot *et al.* (2000) model. Camps *et al.* (2002) modified the Prévot *et al.* (2000) TPW model to account for Atlantic plate motions with the result that the polar shift reduced to approximately 9° from the originally suggested 18°, presumably requiring a less dramatic mantle reorganization event. This revised model is entirely consistent with the North American palaeomagnetic data used by Tarduno & Smirnov (2001). Torsvik *et al.* (2001) also support the existence of a single TPW event since the Early Cretaceous. They regard it as the only feasible explanation for the large difference between the palaeomagnetic and hotspot reconstructions for the North Atlantic. However, they propose that this event occurred over the period 125–95 Ma, rather than instantaneously at ∼110 Ma as favoured by Prévot *et al.* (2000). Using palaeomagnetic data from Pacific seamounts, Sager & Koppers (2000) also found evidence for a short-lived rapid TPW event in the Cretaceous (∼84 Ma) without the need for the 'static hotspot' assumption.

If a significant TPW event, resulting from mass redistribution in the mantle, did occur at *ca.* 110 Ma (Prévot *et al.* 2000) or between 125 and 95 Ma (Torsvik *et al.* 2001) our model predicts that it should be characterized by a peak in the GPFI record that would lag the redistribution event by several million years. The group 2 data set shows no such evidence, with the GPFI peak being observed between 60 and 40 Ma (Figs 4b and 7b). However, evidence of a broad GPFI high is observed in the group 1 data set between 117 and 42 Ma, centred at ∼ 80 Ma (Fig. 7a). This correlates closely with the period of fast TPW identified by Besse & Courtillot (1991) and also with the single TPW events proposed, independently, by Torsvik *et al.* (2001), Prévot *et al.* (2000) and Sager & Koppers (2000). The high mean GPFI for this segment of the GPFI record (Figs 4a and 14) is, ironically, heavily dependent on the high T+RS result of Tarduno *et al.* (2001). Unfortunately, data coverage in this time window is too sparse for the high GPFI suggested by this result to be confirmed as a true feature of GPFI rather than an extreme of PSV. This uncertainty precludes a confirmation of the link with TPW at this stage. This discussion has, again, identified an urgent need for additional GPFI data on the 120–60 Ma time window (Fig. 14). Furthermore, it is important to note that the whole concept of measured TPW must be treated with caution since the premise that hotspots are stationary markers in the mantle is also based on the assumption that they are all plume-derived. While many scientists accept this, there are convincing arguments suggesting that LIPs are spatially controlled by existing lithospheric conditions and have upper-mantle origins (Anderson 1998; Sheth 1999; Smith & Lewis 1999). If, as is claimed by these studies, hotspot trails are a product of progressive lithospheric fissuring, then the method of TPW calculation used by Prévot *et al.* (2000) is, indeed, invalid.

The proposed Palaeozoic avalanching event

An obvious ambiguity in our model lies in the timing of, and geodynamic explanation for, the transition from high to low mean GPFI during the Late Palaeozoic–Early Mesozoic and the temporal extent of the resulting GPFI low. The complete absence of data in the 245–201 Ma window means that it is not possible to confirm whether the GPFI decreased from 325 Ma to a low at ∼250 Ma or at ∼170 Ma. We have chosen, for the purposes of describing stage 2 of our model, to favour a more rapid decrease to low values at around 250 Ma. This choice was based, primarily, on the recognition that the so-called Mesozoic dipole low could have started at around 260 Ma (Perrin & Shcherbakov 1997), coupled with the

Downloaded from https://academic.oup.com/gji/article/152/2/392/653211 by guest on 04 February 2022

tectonic evidence for Pangaea amalgamation (e.g. Eide & Torsvik 1996; Muttoni *et al.* 1996). However, it is accepted that the GPFI decrease may well have been more gradual. Indeed, the notion of the Permo-Triassic singularity (230 ± 5 Ma) for Pangaea (Veevers 1989) tends to favour a model where our stage 3 is unnecessary and stage 2 would have lasted from 350 to 175 Ma. However, this interpretation would not require the existence of a temporally significant MDL, which is contrary to results of well-accepted palaeointensity studies (e.g. Prévot *et al.* 1990; Prévot & Perrin 1992; Perrin & Shcherbakov 1997). Whichever interpretation is eventually favoured by addition of more data, the effect on the overall geodynamic model is negligible. Both options would support a catastrophic avalanching event during the amalgamation of Pangaea, followed by a period of mantle insulation and warming in advance of a period of resumed plate tectonic activity and subduction. Major avalanching events of this nature would undoubtedly be expected to result in counter-flow and it is likely that the effect of such counter-flow, possibly in the form of plumes, would be significant enough to be witnessed in the surface geological record. According to our model episodes of catastrophic avalanching, preceded by ponding at 660 km, are characterized by a rise–peak–fall sequence in the GPFI record. An avalanching event is likely to have an almost instantaneous effect on the heat flow across the CMB (via induced convection as described in Section 6.1) and hence the GPFI. By this reasoning, the actual avalanching event is likely to have occurred a short time before the sharp rise in GPFI. Therefore, the Palaeozoic avalanching event proposed here can be timed at ∼ 350 Ma. The geological record documents potential candidates for surface expressions of counter-flow to this event, such as the existence of greenstones accreted on to continental margins around the Pacific rim (Tatsumi *et al.* 2000). These rocks are radiometrically dated between 350 and 300 Ma and are metamorphosed basalts with geochemical signatures characteristic of hotspot origins. Tatsumi *et al.* (2000) conclude that a large whole-mantle-scale upwelling, similar to that proposed by Larson (1991) for the Cretaceous, occurred beneath the present-day South Pacific between 350 and 300 Ma. They link the Carboniferous event to the onset of the PCRS, noting that the massive amount of energy released had major implications for the Earth system. Alternatively, the counter-flow to the 350 Ma avalanching event may be linked to the later massive outpouring of continental flood basalts associated with the Siberian traps LIP at ∼250–248 Ma and/or the Emeishan traps at 258 Ma. In this case, a significantly longer time period would have elapsed between the avalanching event and its surface signature, which is not entirely consistent with the timescales suggested in our model. The Siberian Traps are believed to result from a plume of deep mantle origin (Basu *et al.* 1995). In our counter-flow explanation, mantle plumes derived from dissociation of D″ are not *required* in the formation of LIPs, though their existence is not in dispute. The dynamics of such rising plumes may well be affected by interaction with global-scale mantle flow, as suggested for the Icelandic plume by Torsvik *et al.* (2001) as a mechanism for dominating the overall tectonic evolution of the North Atlantic. Such global-scale flow could exist as the counter-flow to a major avalanching event.

The proposed Mesozoic/Cenozoic avalanching event

The short-lived episode of high GPFI from 60 to 40 Ma observed in the group 2 data set (Figs 4b and 7b) is, potentially, of great interest in geodynamic terms. Besse & Courtillot (1991) speculated that a hairpin and subsequent standstill in TPW beginning at *ca.* 50 Ma, following a fast period from 110 to 50 Ma, may be linked to the India–Eurasia collision. They note that this tectonic event had a significant effect on lithospheric circulation, being documented in the APW curves of three major continents and linked to the bend in two seamount chains. However, they do not discuss a mechanism. The interpretation presented here, which tentatively proposes a major avalanching event signified by the peak in GPFI between 60 and 40 Ma, lends additional support to the speculation and warrants some discussion. The age of the India–Eurasia collision is still a matter of debate but a best estimate based on a combination of stratigraphic and palaeomagnetic data (Rowley 1996; Powell *et al.* 1988; Jaeger *et al.* 1989; Lee & Lawver 1995) suggests that collision began around 52 Ma. Studies of marine magnetic anomalies clearly show that although India separated from Gondwanaland at 133 Ma, significant northward motion did not start until 96 Ma (Powell *et al.* 1988). The subsequent rapid motion of India, with drift rates ranging from ∼10 to 17 cm yr^{-1}, would have resulted in a latitudinal drift distance of between 5600 and 9200 km by 50 Ma (Treloar & Coward 1991) and subduction of tens of thousands of km^3 of Tethyan lithosphere ahead of the collision. The combination of a hot, low-viscosity mantle (Section 6.2) and the large volume of material present would have generated considerable momentum on subduction. The resulting accumulation at the 660 km boundary layer, would have provided an ideal scenario for avalanching after the resistance of the boundary layer had been overcome. The mechanism for triggering the avalanche may have been, as suggested for the Palaeozoic event in stage 2 of our model, convective removal or detachment of subducting material that has been proposed as a mechanism for initiating the rapid uplift of the Himalayas. Seismic imaging supports the lack of lithospheric mantle below Tibet and the process has firm physical grounding in a scenario where prolonged rapid subduction is followed by continent–continent collision (Hirn *et al.* 1995; England & Molnar 1993). Despite this evidence, our interpretation must be treated as speculative until the existence and timing of the peak in GPFI is unequivocally confirmed by the addition of more data. The inability to accurately constrain the timing of the GPFI peak means that the proposed avalanching event could, conceivably, have taken place earlier in stage 4 of our model. For example, it is possible that avalanching could be linked to the initial stages of Gondwanaland breakup, as suggested by Larson & Kincaid (1996) and supported by the timing of the Cretaceous TPW event (Torsvik *et al.* 2001; Prévot *et al.* 2000). In this case, the response in GPFI may be masked by the data paucity in segment 3 (120–60 Ma) of the record (Fig. 5) again stressing the need to add reliable palaeointensity data in this segment of the record. If the peak in GPFI indeed occurred close to 60 Ma, as suggested in Fig. 7(b) and discussed above, then the counter-flow could possibly have been linked to LIP events such as the Deccan Traps CFB (∼66 Ma) or the North Atlantic Tertiary Igneous Province (61–53 Ma). Alternatively, if, as suggested by the Tarduno *et al.* (2001) result, the GPFI peak occurred closer to 120 Ma, then the avalanching and subsequent mantle reorganization may well have been linked to the extrusion of the Pacific Cretaceous oceanic basalts as proposed by Prévot *et al.* (2000). The extent to which we can interpret the record is limited by the low resolution of the current database. However, these intriguing speculations may well help to direct future palaeointensity work towards enhancing the record in critical time windows, such as between 120 and 60 Ma.

Notwithstanding the ambiguities discussed above, the generic model proposed in Section 6.1 has been successfully tested by its application to documenting the broad evolutionary cycle of Pangaea. This kind of analysis opens up exciting possibilities for future palaeointensity work. Yale & Carpenter (1998) suggested that up to

Downloaded from https://academic.oup.com/gji/article/152/2/392/653211 by guest on 04 February 2022

seven supercontinents (including Pangaea) may have existed since 3 Ga. Broad features in a detailed palaeointensity record extending back to Archaean times would give a key indication of the existence and evolutionary cycles of these transient surface features. Clearly, the paucity of GPFI data prior to 400 Ma means that for such an analysis to take place, a considerable amount of additional palaeointensity work would be required. Furthermore, if palaeointensity is to be used in this geodynamic application, then GPFI measurements contributing to the enhancement of the PINT database must result from studies of geological products of the global geodynamic processes discussed in Section 6. Giant dyke swarms (GDS) provide one example of ideal material in this context. Yale & Carpenter (1998) conclude that GDS are derived directly from mantle sources following supercontinent assembly (Yale & Carpenter 1998) and are therefore products of geodynamic evolution. Their occurrence is widespread throughout the geological record since 3 Ga, they are well-dated (e.g. Ernst & Buchan 1997) and their preservation potential is high owing to the nature of their intrusion into the crust (Yale & Carpenter 1998). They are also known to comprise palaeomagnetically stable material ideal for palaeointensity work and are often emplaced over time periods long enough to average out secular variation (Halls 1986; Halls & Zhang 1998). Palaeointensity studies on this material, using conventional and microwave Thellier techniques to derive T+ estimates, would be invaluable in improving our understanding of the geodynamic evolution of our planet.

8 CONCLUSIONS

The extensive analysis and interpretation of the GPFI record, for the Early Devonian to the Miocene, undertaken in this study has yielded the following conclusions.

(1) GPFI varied on timescales of 10^7–10^8 yr through the period 400–10 Ma, a finding that is not consistent with the conclusions of Selkin & Tauxe (2000). The nature of this variation demonstrates that the lower limit in the range of dipole moment values remains far more constant than the upper limit and, consequently, the mean.

(2) The results produced by segmenting the record according to the dipole moment and age distribution of the data within it provide a very useful reference frame for targeting future palaeointensity studies aimed at addressing current uncertainties in our interpretation.

(3) The 'rock suite' method of grouping data can be used to indicate potential biasing in the record resulting from either over-representation of PSV or systematic non-ideal behaviour exhibited by a batch of samples.

(4) Currently, the best estimate of the long-term variation itself since the Devonian is provided by the segmented group 2 data (Fig. 7b). However, certain parts of the record (those with the highest numbers of CU, ratios of RS/CU and proportions of T+ data) are inevitably more reliable than others. The reliability of the record will be enhanced by adding high-quality palaeointensity estimates where the data coverage is sparse.

(5) No conclusive evidence was obtained to confirm that palaeointensity estimates not derived using the Thellier method with pTRM checks (T+) can systematically bias the dipole moment record. In fact, the distributions of dipole moment in the three data sets used in this study were shown to be startlingly similar, despite having huge disparities in their quantity, age distribution and perceived reliability. This, in itself, suggests that offsets owing to unreliable data in the well-represented parts of the record are likely to be random and cancel one another out.

(6) The filtered absolute palaeointensity record is currently too sparse (particularly in the CNS) to judge, unequivocally, whether mean GPFI and RF are anticorrelated, though a time window analysis tentatively suggests that this may indeed be the case. Nevertheless, it is clear that there is no positive correlation between these parameters.

(7) Long-term variations in GPFI result from a chain of geodynamic processes, beginning with plate reorganizations at the Earth's surface and culminating with changes in the pattern of convection in the outer core. Changes in GPFI are effected almost instantaneously following the catastrophic introduction of cold material into the lower mantle and the resulting increase in convection.

(8) The evolution of GPFI since the Early Devonian can be interpreted in the context of major events in the evolutionary cycle of the supercontinent Pangaea. The four-stage model developed here, featuring two proposed avalanching and mantle reorganization events separated by a period of mantle insulation, is entirely consistent with the observed GPFI variation and is supported by independent lines of evidence from tectonic and seismological studies. The model has ambiguities that will only be fully addressed by the addition of high-quality palaeointensity data in key time periods where data coverage is currently sparse.

(9) An enhanced long-term GPFI record will play a key future role in improving our understanding of the complex relationship between the Earth's core, mantle and crust and its evolution throughout Earth history. Currently, few interpretations are unequivocal owing to key periods of data paucity.

(10) Rigorous palaeointensity studies, targeted particularly at the Archaean–Mid-Palaeozoic age range and the 120–60 Ma time window, should significantly enhance the database and offer the potential to address Earth's early geodynamic evolution and inform the important question of the link between TPW, mantle reorganizations and geomagnetic variation during the Cretaceous. These represent major challenges for future palaeointensity work.

ACKNOWLEDGMENTS

The authors would like to thank Andy Swan of Kingston University for assistance with the statistical analysis. We are grateful to Peter Selkin and Mireille Perrin for valuable reviews of the original manuscript and to two anonymous referees for constructive comments on the geodynamic model. DNT thanks Raymond Hide and Peter Treloar for valuable discussions. We are also grateful to Mireille Perrin for providing a reference list that was used to enhance the PINT database and provide the initial data set for statistical analysis. This work was completed during the course of a NERC-funded studentship and a subsequent KU-funded post-doctoral position to AJB. DNT thanks Kingston University for continued research funding and Stella Bignold for research support.

SUPPLEMENTARY MATERIAL

Supplementary tables are available online from http://www.kingston.ac.uk/esg/labs/biggin.htm

REFERENCES

Anderson, D.L., 1994. Superlumes or supercontinents?, *Geology,* **22,** 39–42.

Anderson, D.L., 1998. The scales of mantle convection, *Tectonophysics,* **284,** 1–17.

Basu, A.R., Poreda, R.J., Renne, P.R., Teichmann, F., Vasiliev, Y.R., Sobolev, N.V. & Turrin, B.D., 1995. High-^{3}He plume origin and

Downloaded from https://academic.oup.com/gji/article/152/2/392/653211 by guest on 04 February 2022

temporal-spatial evolution of the Siberian flood basalts, *Science,* **269,** 822–825.

Besse, J. & Courtillot, V., 1991. Revised and synthetic apparent polar wander paths of the African, Eurasian, North American and Indian plates, and true polar wander since 200 Ma, *J. geophys. Res.,* **96,** 4029–4050.

Brunet, D. & Machatel, P., 1998. Large-scale tectonic features induced by mantle avalanches with phase, temperature and pressure lateral variations in viscosity, *J. geophys. Res.,* **103,** 4929–4945.

Buffet, B.A., 2000. Earth's core and the geodynamo, *Science,* **288,** 2007–2012.

Buffet, B.A., Huppert, H.E., Lister, J.R. & Woods, A.W., 1996. On the thermal evolution of the Earth's core, *J. geophys. Res.,* **101,** 7989–8006.

Calvo, M., Prévot, M., Perrin, M. & Riisager, J., 2002. Investigating the reasons for the failure of palaeointensity experiments: a study on historical lava flows from Mt Etna (Italy), *Geophys. J. Int.*, **149,** 44–63.

Camps, P., Prévot, M., Daignieres, M. & Machetel, P., 2002. Comment on '*Stability of the Earth with respect to the spin axis for the last 130 million years,* ' eds Tarduno, J.A. & Smirnov, A.Y., *Earth planet. Sci. Lett.,* **198,** 529–532.

Cande, S. & Kent, D.V., 1995. Revised calibration of the geomagnetic polarity timescale for the Late Cretaceous and Cenozoic, *J. geophys. Res.,* **100,** 6093–6095.

Cande, S.C., Raymond, C.A., Stock, J. & Haxby, W.F., 1995. Geophysics of the Pitman fracture-zone and Pacific–Antarctic plate motions during the Cenozoic, *Science,* **270,** 947–953.

Coe, R.S., 1967. Palaeointensities of the Earth's magnetic field determined from Tertiary and Quaternary rocks, *J. geophys. Res.,* **72,** 3247–3262.

Coe, R.S., Gromme, C.S. & Mankinen, E.A., 1978. Geomagnetic palaeointensities from radiocarbon dated lava flows on Hawaii and the question of the Pacific non-dipole low, *J. geophys. Res.,* **83,** 1740–1756.

Constable, C., 2000. On rates of occurrence of geomagnetic reversals, *Phys. Earth planet. Inter.,* **118,** 181–193.

Constable, C.G., Tauxe, L. & Parker, R.L., 1998. Analysis of 11 Myr of geomagnetic intensity variation, *J. geophys. Res.,* **103,** 17 735–17 748.

Courtillot, V. & Besse, J., 1987. Magnetic field reversals, polar wander and core–mantle coupling, *Science,* **237,** 1140–1147.

Courtillot, V., Jaupart, C., Manighetti, I., Tapponnier, P. & Besse, J., 1999. On causal links between flood basalts and continental breakup, *Earth planet. Sci. Lett.,* **166,** 177–195.

Cronin, M., Tauxe, L., Constable, C., Selkin, P. & Pick, T., 2001. Noise in the quiet zone, *Earth planet. Sci. Lett.,* **190,** 13–30.

Dalziel, I.W.D., Lawver, L.A. & Murphy, J.B., 2000. Plumes, orogenesis and supercontinental fragmentation, *Earth planet. Sci. Lett.,* **178,** 1–11.

Davies, G.F., 1995. Penetration of plates and plumes through the mantle transition zone, *Earth planet. Sci. Lett.,* **133,** 507–516.

Davies, G.F., 1998. Plates, plumes, mantle convection and mantle evolution, in *The Earth's Mantle: Composition, Structure and Evolution,* pp. 228–229, ed. Jackson, I., Cambridge University Press, Cambridge.

DiVenere, V. & Kent, D.V., 1999. Are the Pacific and Indo-Atlantic hotspots fixed? Testing the plate circuit through Antarctica, *Earth planet. Sci. Lett.,* **170,** 105–117.

Dormy, E, Valet, J-P. & Courtillot, V., 2000. Numerical models of the geodynhamo and observational constraints, *Geochem. Geophys. Geosyst.,*1, paper no. 2000GC000 062.

Eide, E.A. & Torsvik, T.H., 1996. Paleozoic supercontinental assembly, mantle flushing and genesis of the Kiaman superchron, *Earth planet. Sci. Lett.,* **144,** 389–402.

England, P.C. & Molnar, P., 1993. Cause and effect among thrust and normal faulting, anatectic melting and exhumation in the Himalaya, in *Himalayan Tectonics,* Vol. 74, pp. 401–411, eds Treloar, P.J. & Searle, M.P., Geol. Soc. London Spec. Publ.

Ernst, R.E. & Buchan, K.L., 1997. Giant radiating dyke swarms: the use in identifying pre-Mesozoic large igneous provinces and mantle plumes, in *Large Igneous Provinces. Continental, Oceanic and Planetary Flood Volcanism,* Vol. 100, pp. 297–333, eds Mahoney, J.J. & Coffin, M.F., Am. Geophys. Union, Washington, Geophys. Monogr.

Gallet, Y. & Hulot, G., 1997. Stationary and non-stationary behaviour within the geomagnetic polarity timescale, *Geophys. Res. Lett.,* **24,** 1875–1878.

Glatzmaier, G.A., Coe, R., Hongre, L. & Roberts, P.H., 1999. The role of the Earth's mantle in controlling the frequency of geomagnetic reversals, *Nature,* **401,** 885–890.

Goguitchaichvili, A., Prévot, M., Dautria, J.-M. & Bacia, M., 1999. Thermodetrital and crystallodetrital magnetization in an Icelandic hyaloclastite, *J. geophys. Res.,* **104,** 29 219–29 238.

Griffiths, R.W. & Turner, J.S., 1998. Understanding mantle dynamics through mathematical models and laboratory experiments, in *The Earth's Mantle: Composition, Stucture and Evolution,* pp. 191–227, ed. Jackson, I., Cambridge University Press, Cambridge.

Gubbins, D., 1994. Geomagnetic polarity reversals: a connection with secular variation and core–mantle interaction?, *Rev. Geophys.,* **32,** 61–83.

Gubbins, D., 1999. The distinction between geomagnetic excursions and reversals, *Geophys. J. Int.*, **137,** F1–F3.

Gubbins, D. & Zhang, K., 2000. Lateral variations in heat flux around the CMB stabilise the Geodynamo, *EOS, Trans. Am. geophys. Un.,* **81,** Fall Meet. Suppl. 2000, GP62A–02.

Halls, H.C., 1986. Palaeomagnetism, structure and longitudinal correlation of Middle Precambrian dykes from northwestern Ontario and Minnesota, *Can. J. Earth Sci.,* **23,** 142–157.

Halls, H.C. & Zhang, B., 1998. Uplift structure of the southern Kapuskasing zone from 2.45 Ga dike swarm displacement, *Geology,* **26,** 67–73.

Heller, P.L., Anderson, D.L. & Angevine, C.L., 1996. Is the Middle Cretaceous pulse of rapid sea-floor spreading real or necessary?, *Geology,* **24,** 491–494.

Hill, M.J. & Shaw, J., 1999. Palaeointensity results for historic lavas from Mt Etna using microwave demagnetisation/remagnetisation in a modified Thellier experiment, *J. Geophys. Int.,* **139,** 583–590.

Hill, M.J. & Shaw, J., 2000. Magnetic field intensity study of the 1960 Kilauea lava flow, Hawaii, using the microwave palaeointensity technique, *Geophys. J. Int.*, **142,** 487–504.

Hill, M.J., Gratton, M.N. & Shaw, J., 2002. Palaeomagnetic investigation of Tertiary lava from Barrington Tops, NSW, Australia using thermal and microwave techniques, *Earth planet. Sci. Lett.,* **6170,** 1–12.

Hirn, A. *et al.*, 1995. Seismic anisotropy as an indicator of mantle flow beneath the Himalayas and Tibet, *Nature,* **375,** 571–574.

Honda, S., Balachandar, S., Yuen, D.A. & Reuteler, D., 1993. 3-dimensional mantle dynamics with an endothermic phase transition, *Geophys. Res. Lett.,* **20,** 221–224.

Jaeger, J-J., Courtillot, V. & Tapponnier, P., 1989. Palaeontological view of the ages of the Deccan Traps, the Cretaceous/Tertiary boundary and the India–Asia collision, *Geology,* **17,** 316–319.

Johnson, H.P., van Patten, D., Tivey, M. & Sager, W.W., 1995. Geomagnetic polarity reversal frequency for the Phanerozoic, *Geophys. Res. Lett.,* **22,** 231–234.

Jones, G.M., 1977. Thermal interaction of the core and mantle and long-term behaviour of the geomagnetic field, *J. geophys. Res.,* **82,** 1703–1709.

Juárez, M.T., Tauxe, L., Gee, J.S. & Pick, T., 1998. The intensity of the Earth's magnetic field over the past 160 million years, *Nature,* **394,** 878–881.

Kono, M. & Tanaka, H., 1995. Intensity of the geomagnetic field in geological time: a statistical study, in *The Earth's Central Part: it's Structure and Dynamics,* pp. 75–94, ed. Yukutake, T., Terrapub, Tokyo.

Kosterov, A.A. & Prévot, M., 1997. Possible mechanisms causing failure of Thellier palaeointensity experiments in some basalts, *Geophys. J. Int.*, **134,** 554–572.

Kruiver, P.P., Dekkers, M.J. & Langereis, C.G., 2000. Secular variation in Permian red beds from Dome de Barrot, SE France, *Earth planet. Sci. Lett.,* **179,** 205–217.

Larson, R.L., 1991. Latest pulse of Earth: evidence for a Mid-Cretaceous superplume, *Geology,* **19,** 547–550.

Larson, R.L. & Kincaid, C., 1996. Onset of Mid-Cretaceous volcanism by elevation of the 670 km thermal boundary layer, *Geology,* **24,** 551–554.

Larson, R.L. & Olson, P., 1991. Mantle plumes control magnetic reversal frequency, *Earth planet. Sci. Lett.,* **107,** 437–447.

Lay, T., Williams, Q. & Garnero, E.J., 1998. The core–mantle boundary layer and deep Earth dynamics, *Nature,* **392,** 461–468.

Lee, T.Y. & Lawver, L.A., 1995. Cenozoic plate reconstruction of Southeast Asia, *Tectonophysics,* **251,** 85–138.

Downloaded from https://academic.oup.com/gji/article/152/2/392/653211 by guest on 04 February 2022

Loper, D.E., 1992. On the correlation between mantle plume flux and the frequency of reversals of the geomagnetic field, *Geophys. Res. Lett.,* **19,** 25–28.

Loper, D.E. & McCartney, K., 1986. Mantle plumes and the periodicity of magnetic-field reversals, *Geophys. Res. Lett.,* **13,** 1525–1528.

Machatel, P. & Weber, P., 1991. Intermittent layered convection in a model mantle with an endothermic phase change at 670 km, *Nature,* **350,** 55–57.

McFadden, P.L. & McElhinny, M.W., 1982. Variations in the geomagnetic dipole 2: statistical analysis of VDMs for the past 5 million years, *J. Geomag. Geoelectr.,* **34,** 163–189.

McFadden, P.L. & Merrill, R.T., 1986. Geodynamo energy source constraints from paleomagnetic data, *Phys. Earth planet. Inter.,* **43,** 22–33.

McFadden, P.L. & Merrill, R.T., 1995. History of Earth's magnetic field and possible connections to core–mantle boundary processes, *J. geophys. Res.,* **100,** 307–316.

McFadden, P.L. & Merrill, R.T., 1997. Asymmetry in the reversal frequency before and after the Cretaceous normal polarity superchron, *Earth planet. Sci. Lett.,* **149,** 43–47.

McFadden, P.L. & Merrill, R.T., 2000. Evolution of the geomagnetic reversal frequency since 160 Ma: is the process continuous?, *J. geophys. Res.,* **105**, 28 455–28 460.

Merrill, R.T., McElhinny, M.W. & McFadden, P.L., 1996. *The Magnetic Field of the Earth: Palaeomagnetism, the Core and the Deep Mantle,* p. 531, Academic Press, London.

Muttoni, G., Kent, D.V. & Channell, J.E.T., 1996. Evolution of Pangea: paleomagnetic constraints from the Southern Alps, Italy, *Earth planet. Sci. Lett.,* **140,** 97–112.

Opdyke, N.D. & Channell, J.E.T., 1996. *Magnetic Stratigraphy,* p. 346, Academic Press, London.

Perrin, M. & Shcherbakov, V., 1997. Palaeointensity of the Earth's magnetic field for the past 400 Ma: evidence for a dipole structure during the Mesozoic low, *J. Geomag. Geoelectr.,* **49,** 601–614.

Perrin, M., Schnepp, E. & Shcherbakov, V., 1998. Palaeointensity database updated, *EOS, Trans. Am. geophys. Un.,* **79,** 198.

Pick, T. & Tauxe, L., 1993. Geomagnetic palaeointensities during the Cretaceous Normal Superchron measured using submarine basaltic glass., *Nature,* **366,** 238–242.

Powell, C.McA., Roots, S.A. & Veevers, J.J., 1988. Pre-break up and continental extension in East Gondwanaland and the early opening of the eastern Indian Ocean, *Tectonophysics,* **155,** 261–283.

Prévot, M. & Perrin, M., 1992. Intensity of the Earth's magnetic field since Precambrian time from Thellier-type intensity data and inferences on the thermal history of the core, *Geophys. J. Int.,* **108,** 613–620.

Prévot, M., Mankinen, E., Coe, R.S. & Grommé, C.S., 1985. The Steens Mountain (Oregon) geomagnetic polarity transition 2. Field intensity variation and discussion of reversal models, *J. geophys. Res.,* **90,** 10 417–10 448.

Prévot, M., Derder, M.E., McWilliams, M. & Thompson, J., 1990. Intensity of the Earth's magnetic field—evidence for a Mesozoic dipole low, *Earth planet. Sci. Lett.,* **97,** 129–139.

Prévot, M., Mattern, E., Camps, P. & Daignieres, M., 2000. Evidence for a 20° titling of the Earth's rotation axis 110 million years ago., *Earth planet. Sci. Lett.,* **179,** 517–528.

Ricard, Y., Richards, M., Lithgowbertelloni, C. & Lestunff, Y., 1993. A geodynamic model of mantle density heterogeneity, *J. geophys. Res.,* **98,** 21 895–21 909.

Ricou, L.E. & Gibert, D., 1997. The magnetic reversal sequence studied using wavelet analysis: a record of the Earth's tectonic history at the core–mantle boundary, *Géophysique Interne,* **325,** 753–759 (English translation).

Rolph, T.C. & Shaw, J., 1985. A new method of palaeofield magnitude correction for thermally altered samples and its application to lower Carboniferous lavas, *Geophys. J. R. astr. Soc.,* **80,** 773–781.

Rowley, D.B., 1996. Age of initiation of collision between India and Asia: a review of stratigraphic data, *Earth planet. Sci. Lett.,* **145,** 1–13.

Russell, S.A., Lay, T. & Garnero, E.J., 1998. Seismic evidence for small-scale dynamics in the lowermost mantle at the root of the Hawaiian hotspot, *Nature,* **396,** 255–258.

Sager, W.W. & Koppers, A.A.P., 2000. Late Cretaceous polar wander of the Pacific plate: evidence of a rapid true polar wander event, *Science,* **287,** 455–459.

Sarson, G.R., 2000. Reversal models from dynamo calculations, *Phil. Trans. R. Soc. Lond.,* A, **358,** 921–942.

Selkin, P.A. & Tauxe, L., 2000. Long-term variations in palaeointensity, *Phil. Trans. R. Soc. Lond.,* A, **358,** 1065–1088.

Shaw, J., 1974. A new method of determining the magnitude of the palaeomagnetic field, application to five historic lavas and five archaeological samples, *Geophys. J.R. astr. Soc.,* **39,** 133–141.

Sheth, H.C., 1999. Flood basalts and large igneous provinces from deep mantle plumes: fact, fiction and fallacy, *Tectonophysics,* **311,** 1–29.

Smith, P.J., 1967. The intensity of the Tertiary geomagnetic field, *Geophys. J. R. astr. Soc.,* **12,** 239–258.

Smith, A.D. & Lewis, C., 1999. The planet beyond the plume hypothesis, *Earth Sci. Rev.,* **48,** 135–182.

Steinberger, B., 2000. Plumes in a convecting mantle: Models and observation for individual hotspots, *J. geophys. Res.,* **105,** 11 127–11 152.

Steinberger, B. & O'Connell, R.J., 1998. Advection of plumes in mantle flow: implications for hotspot motion, mantle viscisity and plume distribution, *Geophys. J. Int.*, **132,** 412–434.

Tackley, P.J., 2000. Mantle convection and plate tectonics: towards and integrated physical and chemical theory, *Science,* **288,** 2002–2006.

Tackley, P.J., Stevenson, D.J., Glazmaier, G.A. & Schubert, G., 1993. Effects of an endothermic phase transition at 670 km depth in a spherical model of convection in the Earth's mantle, *Nature,* **361,** 699–704.

Tanaka, H., Kono, M. & Uchimura, H., 1995. Some global features of palaeointensity in geological time, *Geophys. J. Int.,* **120,** 97–102.

Tarduno, J.A. & Smirnov, A.V., 2001. Stability of the Earth with respect to the spin axis for the last 130 million years, *Earth planet. Sci. Lett.,* **184,** 549–553.

Tarduno, J.A. & Smirnov, A.V., 2002. Response to comment on 'Stability of the Earth with respect to the spin axis for the last 130 million years,' by Camps, P., Prévot, M., Daignieres, M. & Machetel, P., *Earth planet. Sci. Lett.,* **198,** 533–539.

Tarduno, J.A., Cottrell, R.D. & Smirnov, A.V., 2001. High geomagnetic intensity during the Mid-Cretaceous from Thellier analyses of single plagioclase crystals, *Science,* **291,** 1779–1783.

Tatsumi, Y., Tomomi, K., Ishizuka, H., Maruyama, S. & Nishimura, Y., 2000. Activation of Pacific mantle plumes during the Carboniferous: evidence from accretionary complexes in southwest Japan, *Geology,* **28,** 580–582.

Tauxe, L. & Hartl, P., 1997. 11 million years of Oligocene geomagnetic field behaviour, *Geophys. J. Int.*, **128,** 217–229.

Thellier, E. & Thellier, O., 1959. Sur l'intensité du champ magnétique terrestre dans la passé historique et géologique, *Ann. Géophys.,* **15,** 285–376.

Thomas, D.N., 1992. Rock magnetic and palaeomagnetic investigations of the Precambrian Gardar lava succession, South Greenland, *PhD thesis,* University of Liverpool, Liverpool.

Thomas, D.N., Rolph, T.C. & Friel, D.F., 1997. Permo-Carboniferous (Kiaman) palaeointensity estimates from the western Bohemian massif, *Geophys. J. Int.*, **130,** 257–265.

Thomas, D.N., Rolph, T.C., Shaw, J., de Sherwood, S.G. & Zhuang, Z., 1998. Palaeointensity studies of a Late Permian lava succession from Guizhou Province, South China: implications for post-Kiaman dipole field behaviour, *Geophys. J. Int.*, **134,** 856–866.

Thomas, D.N., Biggin, A.J. & Schmidt, P.W., 2000. A palaeomagnetic study of Jurassic intrusives from southern New South Wales: further evidence for a pre-Cenozoic dipole low, *Geophys. J. Int.*, **140,** 621–635.

Thomas, N., 1993. An integrated rock magnetic approach to the selection or rejection of ancient basalt samples for palaeointensity experiments, *Phys. Earth planet. Inter.,* **75,** 329–342.

Torsvik, T.H., Trench, A., Lohmann, K.C. & Dunn, S., 1995. Lower Ordovician reversal asymmetry: an artifact of remagnetisation or nondipole field disturbance?, *J. geophys. Res.,* **100,** 17 885–17 898.

Torsvik, T.H., Mosar, J. & Eide, E.A., 2001. Cretaceous–Tertiary geodynamics: a North Atlantic exercise, *Geophys. J. Int.*, **146,** 850–866.

Treloar, P.J. & Coward, M.P., 1991. Indian plate motion and shape: constraints on the geometry of the Himalayan orogen, *Tectonophysics,* **191,** 189–198.

Downloaded from https://academic.oup.com/gji/article/152/2/392/653211 by guest on 04 February 2022

Trompert, R. & Hansen, U., 1998. Mantle convection simulations with rheologies that generate plate-like behaviour, *Nature,* **395,** 686–689.

Veevers, J.J., 1989. Middle-late Triassic (230 ± 5 Ma) singularity in the stratigraphic and magmatic history of the Pangean heat anomaly, *Geology,* **17,** 784–787.

Vogt, P.R., 1972. Evidence for global synchronism in mantle plume convection and possible significance to geology, *Nature,* **240,** 338–342.

Walton, D., Shaw, J., Share, J.A. & Hakes, J., 1992. Microwave demagnetisation, *J. Appl. Phys.,* **71,** 1549–1551.

Walton, D., Share, J.A., Rolph, T.C. & Shaw, J., 1993. Microwave magnetisation, *Geophys. Res. Lett.,* **20,** 109–111.

Walton, D., Snape, S., Rolph, T.C., Shaw, J. & Share, J.A., 1996. Application of ferrimagnetic resonance heating to palaeointensity determinations, *Phys. Earth planet. Inter.,* **94,** 183–186.

Wen, L.X. & Anderson, D.L., 1995. The fate of slabs inferred from seismic tomography and 130 million years of subduction, *Earth planet. Sci. Lett.,* **133,** 185–198.

Yale, L.B. & Carpenter, S.J., 1998. Large igneous provinces and giant dyke swarms: proxies for supercontinent cyclicity and mantle convection, *Earth planet. Sci. Lett.,* **163,** 109–122.

Yuen, D.A., Cadek, O.P., Boehler, R., Moser, J. & Matyska, C., 1994. Large cold anomalies in the deep mantle and mantle instability in the Cretaceous, *Terra Nova,* **6,** 238–245.

Zhang K. & Gubbins, D., 2000a. Is the geodynamo process intrinsically unstable?, *Geophys. J. Int.*, **140,** F1–F4.

Zhang K. & Gubbins, D., 2000b. Scale disparities and magnetohydrodynamics in the Earth's core, *Phil. Trans. R. Soc. Lond.,* A, **358,** 899–920.

Downloaded from https://academic.oup.com/gji/article/152/2/392/653211 by guest on 04 February 2022